TEST AND EVALUATION OF ULTRASONIC ADDITIVE MANUFACTURING (UAM) FOR A LARGE AREA MAINTENANCE SHELTER (LAMS) BASEPLATE

THESIS

Daniel H. Gartland, Captain, USAF

AFIT-ENV-MS-15-M-158

DEPARTMENT OF THE AIR FORCE
AIR UNIVERSITY

AIR FORCE INSTITUTE OF TECHNOLOGY

Wright-Patterson Air Force Base, Ohio

AFIT-ENV-MS-15-M-158

TEST AND EVALUATION OF ULTRASONIC ADDITIVE MANUFACTURING FOR A LARGE AREA MAINTENANCE SHELTER (LAMS) BASEPLATE

THESIS

Presented to the Faculty

Department of Systems and Engineering Management

Graduate School of Engineering and Management

Air Force Institute of Technology

Air University

Air Education and Training Command

In Partial Fulfillment of the Requirements for the

Degree of Master of Science in Engineering Management

Daniel H. Gartland, MS, PMP

Captain, USAF

March 2015

Abstract

Additive manufacturing is an exciting new manufacturing technology that could have application to Air Force Civil Engineer (CE) operations. This research replicates a Large Area Maintenance Shelter (LAMS) baseplate design for ultrasonic additive manufacturing (UAM). Due to production problems the test section was not built as designed. Instead, a smaller block of material was submitted for evaluation. After the UAM build, ultrasonic inspection was conducted to identify anomalies in the test piece.

The results of this proof of concept study indicate that UAM is not yet ready for CE expeditionary applications requiring a high degree of mechanical strength. The machine failed to build a baseplate of the same dimensions as would be required for use in the field. Further, the test specimen produced using UAM had a substantial number of anomalies throughout the entire *y*-axis of orientation. As the technology continues to improve, UAM may produce welds of sufficient strength to support expeditionary structural applications.

This project is dedicated to the Suze because she is hours of entertainment, and never fails to raise the spirits of those in the room.

Acknowledgments

I would like to acknowledge my advisor, Maj Valencia who provided me the opportunity to conduct this research and granted me the latitude to accomplish it to the conclusion. Your support is appreciated and I learned a lot from you throughout the process. Maj Freels guided me throughout the mechanics of materials portions my research and showed me how to solve problems more like a scientist. Dr. Wander's quick and insightful feedback was instrumental to my completion of the document. The 49 Material Maintenance Squadron at Holloman AFB, specifically TSgt Mingo, SSgt Tanaka, and SrA Brooks provided me their expertise about expeditionary structures and took the time to walk me through the pieces in their kits. The Ohio State University Smart Materials Lab under Professor DaPino and his student Matt Scheidt were important to this research and their continued partnership with AFIT will benefit many students in the future. AFRL's Non-Destructive Evaluation division under Dr. Brausch and Dan Laufersweiler provided timely evaluations and explanations of the methods used and this research could not have been accomplished without them.

Daniel H. Gartland

Table of Contents

Page

List of Figures

List of Tables

Page

TEST AND EVALUATION OF ULTRASONIC ADDITIVE MANUFACTURING (UAM) FOR A LARGE AIRCRAFT MAINTENANCE SHELTER (LAMS) BASEPLATE

I. Introduction

General Issue

The traditional manufacturing process is an assembly line that takes a uniform block of material and machines it to a shape required for some other assembly line process. Eventually, enough sub-components are assembled to form a usable product. Another traditional manufacturing process is casting liquid metals or composites into a particular shape using a mold. Because liquid metal can fill the unique geometries inside of a mold, casting has filled the role of creating complex shaped sub-components which are difficult to machine. A new manufacturing process is emerging called additive manufacturing (AM) and its beginnings can be traced to the 1980s. AM, as opposed to subtractive manufacturing, builds a design up layer by layer into a component saving time and machining cost in addition to granting a wide degree of freedom in designing customized parts for machines. To that end, potential applications for AM may exist in the U.S. Air Force (AF) to support a wide variety of operations throughout the world.

AF operations are global and expeditionary and that expeditionary infrastructure equipment is aging. Supplies to repair aged infrastructure frequently take a long time to arrive and, in a deployed environment, this can lead to significant risk to the mission, personnel, and schedule. Two AF core competencies are Agile Combat Support and Rapid Global Mobility. The Base Expeditionary Airfield Resources (BEAR) equipment set enable and support these core competencies. The BEAR equipment kit can include

small, medium, and large shelters composed of many parts subjected to a wide range of environmental and use conditions. As AM technology matures, the availability of the technology has potential application to Air Force Civil Engineer (CE) operation and maintenance of air base infrastructure. AM functions in the same manner as conventional printing except, instead of depositing ink on a sheet of paper, objects are created through depositing very thin layers of material. Over time, a three dimensional (3D) object is built up (Brynjolfsson & McAfee, 2014: 36). This method of construction offers many advantages due to the control a designer can implement in the voids and channels of the object. AM also offers the potential to rapidly prototype components that are critical to meeting the organizational objectives which logistic and time constraints would otherwise make difficult (Gibson, Rosen, & Stucker, 2010: 1). Ultrasonic additive manufacturing (UAM), a technology whereby an object is built up in metal foil layers may present a resource-effective approach to maintaining BEAR equipment deployed at austere locations.

Problem Statement

This research investigates the strength of a large area maintenance shelter (LAMS) baseplate constructed through UAM of Aluminum 6061 (Al-6061) compared to a cast Aluminum 356.0 (A356.0) composite baseplate normally used. Al-6061 is a welding grade aluminum frequently used in the manufacturing industry and has been found to be compatible with the UAM process (Wolcott, Hehr, & Dapino, 2014: 2056). On the other hand, A356.0 is used to manufacture LAMS baseplates because of its low cost and favorable strength properties which allow the LAMS to meet applicable building

codes (Kane, 2014). Conducting non-destructive evaluation (NDE) on prototype components provides information to the CE career field prior to implementing a more costly, full-scale program.

Research Objectives/Questions/Hypotheses

The objective of this research is to determine the feasibility of using UAM to produce a LAMS baseplate. As such, the overarching research question is posed as: Is a LAMS baseplate produced by UAM as robust as traditionally manufactured samples? In support of the primary research question, a cost comparison between the UAM production and the cast LAMS baseplate will be accomplished to further quantify feasibility.

Methodology

The overall methodology compares a UAM produced LAMS baseplate test section to one A356.0 cast LAMS baseplate test section. A set of assumptions were drafted based on subject matter expert input and data in published literature. These assumptions are explained in greater detail in Chapter Three. Based on 49th Material Maintenance Squadron (49 MMS) Craftsman input, the LAMS baseplate was identified as a high failure component in the BEAR expeditionary kit that could be modeled using an open-source 3D computer aided design (CAD) software. The Ohio State University Smart Materials and Structures Lab produced one Al-6061 cube for comparison in the experiment. Non-destructive evaluation (NDE) was conducted on each sample by the Air Force Research Laboratory (AFRL) which can be used to improve future designs. This

study inspects the test sections for anomalies for evidence of possible fracture as suggested by the 49 MMS Craftsman. Given the manufacturing technique of UAM, there is potential for delamination in the UAM produced component resulting in a shear failure mode as well.

Assumptions/Limitations

Due to the high cost of UAM production at this time, the LAMS baseplate was modeled in a test section and was scanned using nondestructive evaluation inspection methods. Since the ultrasonic inspection equipment could not produce an adequate scan of the cast baseplate an assumed value of 90% was assigned to the baseline cast test section for comparison with the UAM produced test section. Assumptions associated with design and testing of the UAM produced baseplate are detailed further in Chapter Two and Three.

Implications

The implications of this research to the CE career field include revolutionizing the expeditionary supply chain process through dramatic reduction of materiel acquisition time. Reduction in procurement time manifests into shorter down time for structures affected by a failed component. Further, the career field could realize a reduction in the amount of deployable bench stock needed to support global operations. Finally, UAM may provide expeditionary infrastructure maintenance solutions to problems not yet identified.

Document Overview

Following this introduction this study is organized in the traditional five chapter thesis format. Chapter Two contains a literature review of relevant publications in AM and materials. Several books are reviewed for design considerations and production technique. UAM is further defined and explained. The literature review concludes by providing historical and contextual background of AM technology and its implications to the CE mission.

Chapter Three explains the overall experiment structure and method used in the research. The assumptions employed in the experiment are also justified in the literature review. The use of NDE is presented and the general build conditions are discussed. The comparison between the cast A356.0 baseplate and the UAM produced test specimen is reviewed. Measures chosen for evaluation are further discussed as part of the experiment's description.

Chapter Four contains results from the experiment and in-depth discussion on their interpretation. The findings from the testing are compared side-by-side, and the implications for expeditionary CE operations are explained. The percentage of usable weld quality is presented. Additionally, this chapter discusses how the results may be incorporated into a pilot study of the capability for use in the Prime Base Expeditionary Emergency Force (Prime BEEF) Unit Type Codes (UTC)s.

Chapter Five summarizes the research and discusses the implications for the CE community. The information contained in this chapter provides decision makers with the knowledge to support further research into the application and possible inclusion of AM

capability into the Prime BEEF UTCs. Additionally, areas for potential improvement of UAM design and future study are suggested.

II. Literature Review

Chapter Overview

This chapter includes a survey of the relevant literature related to additive manufacturing (AM) applications to Civil Engineer (CE) expeditionary operations. The chapter begins with the history of AM and continues to the development of Ultrasonic Additive Manufacturing (UAM) technology. Design techniques for AM are also discussed with emphasis towards the production of the Large Area Maintenance Shelter (LAMS) baseplate. AM processes are limited by technical boundaries of the structures and characteristics desired in the part to be built (Smyth, 2013: 22). The chapter also discusses the ideas of the systems engineering "-ilities", specifically robustness as it relates the UAM produced baseplate.

History

The very beginning of AM can be traced back to over 100 years to topographic and photosculpture techniques pioneered by Blanther and Perera to produce contour relief maps (Bourell, Beaman, Leu, & Rosen, 2009: 5). The present state of AM can be traced back to the mid 1980s with the propagation of sterolithography. This sparked the development of numerous other AM processes to the present day (International Solid Freeform Fabrication Symposium, 2009: 1). The spread of desktop computers, a growing global economy, and increasing availability of laser technology are all enablers of the continued growth of the AM field (International Solid Freeform Fabrication Symposium, 2009: 1). The early 1990s saw the development of numerous AM technologies such as:

laser sintering, lamination, fused deposition modeling, and binder jetting (International Solid Freeform Fabrication Symposium, 2009: 1).

AM is a process of joining two materials to make objects from three-dimensional (3D) model data, usually layer by layer (Kuhn & Collier, 2014). AM has application in a wide range of disciplines from medical to aerospace, all of which continue to drive development in the field. The applications of AM appear to be limited by only two things: the ingenuity of designers and engineers employing the technology and the properties of the materials developed by chemists and material scientists. Parts produced through AM maybe custom, unique pieces for patients in a hospital or could serve as replacement components on aircraft or naval ships. In particular AM excels at creating one of a kind, channelized structures for incorporation into an existing system (Kuhn & Collier, 2014).

AM may reduce the production time of complex 3D objects from a computer-aided design (CAD) software package. Part-count reduction is achieved through constructing an entire component at one time instead of machining several different subcomponents in an assembly line (Kuhn & Collier, 2014). The Department of Defense (DOD) acquisition community suggests that AM presents an opportunity to reduce, or perhaps eliminate, the traditional supply chain management system through the reduction of bench stock and lead times for procurement (Brown, Davis, Dobson, & Mallicoat, 2014: 8). Regarding the benefits of AM, Brown, Davis, Dobson, and Mallicoat highlight: "There is speed (design to production), flexibility, and elimination of production run requirements (economies of scale), and what is sure to be far-reaching effects on transportation pipelines" (2014: 8). The DoD has also identified cost savings, improved

sustainment, increased combat readiness, personnel reductions, and quality improvement as potential benefits of AM implementation (Freitag, Wohlers, & Philippi, 2003: 10). AM breaks from traditional manufacturing methods as it does not require a detailed analysis of part geometry to determine the sequence of which different features are fabricated and tools and tasks are required (Gibson, Rosen, & Stucker, 2010:2).

AM Technology

There are seven different types of AM technology which may be classified into three categories: powder bed processes, polymers, and other metals/polymers (Kuhn & Collier, 2014). The classifications are based on the American Society for Testing and Materials (ASTM) standard terminology for AM technology. This section provides an overview of each technology within its respective category. Table 1 is a summary of the different AM technology processes and types.

Table 1. Summary of AM Technology

Powder Bed Processes	Polymers	Other Metal/Polymer
Selective Laser Melting	Vat Photopolymerization	Sheet Lamination
Selective Mask Sintering	Material Extrusion	
Selective Laser Sintering	Material Jetting	
Electron Beam Melting		
Binder Jetting		
Directed Energy Deposition		

Powder Bed Processes

Powder bed processes can be further categorized into three more specific processes: powder bed fusion, binder jetting, and directed energy deposition. Powder bed fusion is an additive manufacturing process in which thermal energy selectively fuses regions of a powder bed (ASTM International, 2012: 1). Powder bed fusion includes laser processes such as selective laser melting (SLM) selective mask sintering (SMS) which manufacture metal, selective laser sintering (SLS) which works on polymers, and electron beam melting for metals. The benefits of the laser processes used in powder bed fusion are gained through the high degree of accuracy of the build owing to its nature as a vector operation (Kuhn & Collier, 2014). By vector operation, the laser focuses on specific points rather than a broad area.

The second category binder jetting is an additive manufacturing process in which a liquid bonding agent is selectively deposited to join powder materials (ASTM International, 2012: 1). In plain terms, binder jetting can be pictured as "gluing" the build material together to create a structure.

Finally, directed energy deposition is an additive manufacturing process wherein focused thermal energy is used to fuse material as they are deposited on a build surface (ASTM International, 2012: 1). Examples include powder feed, and wire feed which both use metals as their material. Deposition modeling has potential application in the field of material repairs of aging effects such as crack repair (Kuhn & Collier, 2014). It also shares many similarities to traditional welding but gains advantage through the consistency of a machine operating the weld as opposed to a technician.

Polymers

The second major category of AM processes, Polymers, can be organized into three categories: vat photopolymerization, material extrusion, and material jetting. Vat photopolymerization is a process in which liquid photopolymer in a vat is selectively cured by light activated polymerization (ASTM International, 2012: 2). This is a complex chemical reaction where some type of radiation, gamma rays, x-rays, electron beams, ultraviolet, and visible light is applied to the build material to cure it in a specific shape (Gibson, Rosen, & Stucker, 2010: 61). Vat photopolymerization includes steriolithography (SLA), flash curing, and film transfer imaging (FTI). Potential applications of this technology are distinct in the ability to rapidly prototype components for use in other projects.

Material Extrusion is an additive manufacturing process in which material is selectively dispensed through a nozzle or orifice (ASTM International, 2012: 1). Fused deposition modeling (FDM) is an example of material extrusion and is a widespread form of rapid prototyping used in many industries. FDM is often the most recognized form of AM owing largely to its widespread home use by consumers. It is best conceptualized as a hot glue gun following a prescribed design path for each layer to construct the build.

Finally, material jetting is an additive manufacturing process in which droplets of build material are selectively deposited (ASTM International, 2012: 2). Drop on demand and multijet modeling are examples of material jetting.

Other Metal/Polymer

The final major AM process is generically titled other metal/polymer. This research focuses on the sheet lamination process where layers of material are bonded to

form an object (ASTM International, 2012: 1). The sheet lamination process welds metal strips with glue, heat, or high frequency sound. Ultrasonic additive manufacturing (UAM) is a sheet lamination process and is unique from the other processes because it has a low thermal load and may be used to imbed sensors and probes during the construction. UAM is explained further in the next section. Often, lamination processes yield a build which requires further machining in order to render a useful component. UAM is promising for welding different materials and embedding sensors or probes within a component (Wolcott, Hehr, & Dapino, 2014: 2055)

UAM Technology

This section discusses UAM in more detail and includes its benefits, process parameters, and known limitations. UAM is a hybrid sheet laminating process that combines ultrasonic seam welding and computer numerical controlled (CNC) milling into one machine for manufacturing. Solidica, Inc. first patented and commercialized the UAM process in 2000 (White, 2000). Fabrisonic, LLC, a joint venture between Solidica and the Edison Welding Institute (EWI) is a major manufacture of UAM systems.

There are several benefits which may be gained from application of UAM the first of which is the capability to eliminate the manufacturing chain and produce components in one step from design to production (Fabrisonic LLC, 2014). UAM produces components through solid state bonding which has numerous advantages. This low thermal loading is an advantage the UAM machines have over other AM technologies (DaPino, 2014). Each layer is composed of several metal foils placed side-by-side and built from the bottom to the top as shown in (Gibson, Rosen, & Stucker, 2010: 215).

Four layers of foil are deposited in one level during the UAM process. After deposition, a CNC milling head shapes each level into the computer specified shape and contour resulting in a smooth surface finish with tolerances down to 0.0005 inches (Gibson, Rosen, & Stucker, 2010: 216) (Fabrisonic LLC, 2014).

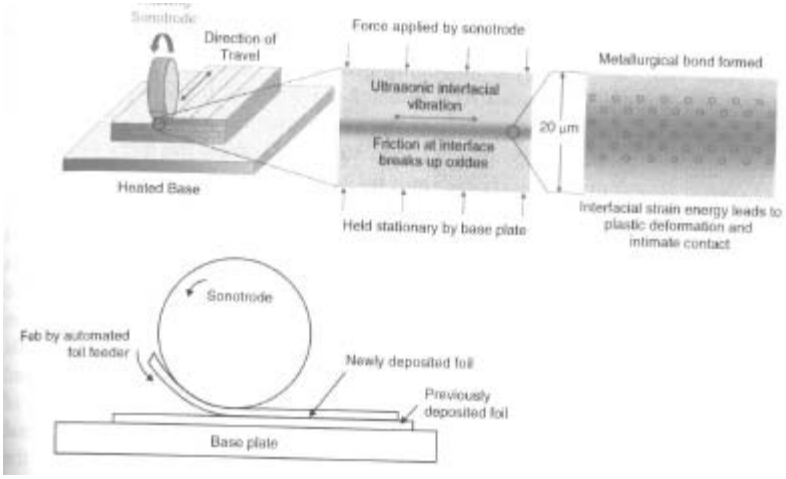

Figure 1. UAM Schematic (Gibson, Rosen, & Stucker, 2010: 215)

Another benefit obtained from UAM is the unique capability to embed different materials and sensors as part of the build process. The machine can change out build material and other process parameters as part of the production. Further, it also possesses the ability to join dissimilar materials, such as copper and aluminum. The use of CNC milling and cutting eliminates the dependence on layer thickness for accuracy encountered in other AM processes (Gibson, Rosen, & Stucker, 2010: 215)

The process parameters which most greatly affect the production through UAM are vibration amplitude, normal force, welding speed, and layer surface roughness (Obielodan, Janaki Ram, Stucker, & Taggart, 2010: 06-1). These parameters are

controllable by the operator to ensure minimal detrimental impact to bond qualities and strength (Gibson, Rosen, & Stucker, 2010: 220). Other researchers identified vibration amplitude as the most significant parameter in a UAM build (Wolcott, Hehr, & Dapino, 2014: 2062).

Vibration amplitude in general increases the amount of energy delivered to the build and results in elastic/plastic deformation at the materials interface which produces a higher quality weld (Gibson, Rosen, & Stucker, 2010: 220). An optimum oscillation amplitude exists for a discrete material thickness, geometry, and combination of materials which produces enough energy to achieve plastic deformation and fill the voids due to surface roughness of the materials (Gibson, Rosen, & Stucker, 2010: 220). Bonding does deteriorate if the energy input exceeds a critical level and can damage previously formed bonds at the weld interface due to excessive stress/fatigue (Gibson, Rosen, & Stucker, 2010: 220).

The normal force is the load applied on the build material by the sonotrode and is required to ensure the ultrasonic energy is delivered to the foils to establish bonds throughout the interface (Gibson, Rosen, & Stucker, 2010: 220). Normal forces higher or lower than the optimum level degrade the quality of the bonds and reduces the linear weld density the bond obtains (Gibson, Rosen, & Stucker, 2010: 220). Thus the normal force is essentially a stabilizing force to keep the production in place to allow uniform power application from the sonotrode.

The welding speed refers to the time it takes for the sonotrode to travel across each layer of production. This weld exposure time has a direct effect on the bond strength in the UAM production (Gibson, Rosen, & Stucker, 2010: 221). At higher

welding speeds, contact time between the sonotrode and build material is reduced producing an insufficient amount of weld exposure for the area (Janaki, Yang, & Stucker, 2006: 231). For this same reason lower welding speeds can produce extremely high weld densities however there is an increased risk for metal fatigue and damage to previously formed bonds (Gibson, Rosen, & Stucker, 2010: 221). Other drawbacks to the lower weld speed settings are increased part production time which may lead to a higher project cost (Janaki, Yang, & Stucker, 2006: 234).

Finally, layer surface roughness is often identified as a major source of anomalies and defects in the bonding layers (Janaki, Yang, & Stucker, 2006: 225). The reduce the effect of layer surface roughness on a build, an intermediate step where the sonotrode machines each layer as it is applied to the part under construction (Janaki, Yang, & Stucker, 2006: 234). The interlayer defects shown in Figure 2, can be minimized through the incorporation of intermediate surface texturing throughout the build.

The UAM process also has limitations. First, it consumes a significant amount of material for each pass and has to machine unique contours in the production process. During each build there is a "transient region" wherein the sonotrode first contacts the build surface creating a slightly more variable weld before reaching uniformity further along its axis of movement. This implies each pass must be a straight line of a fixed interval during the entire build to prevent adjacent layer defects in the foils discussed later in this section (Obielodan, Janaki Ram, Stucker, & Taggart, 2010: 06-7). The defects which arise during the UAM process may be categorized as type one, or interlayer and type two, or adjacent foil defects (Obielodan, Janaki Ram, Stucker, & Taggart, 2010: 06-1). Minimizing defects in the UAM process is critical to the ability to

use a manufactured part in a structural load bearing capacity. Figure 2 and Figure 3 provide illustrations of these defects.

Much attention has been devoted to minimizing interlayer and adjacent weld defects. Methods suggested to reduce the number of interlayer defects are slower weld speed and increase the amount of energy transfer to the build surface (Obielodan, Janaki Ram, Stucker, & Taggart, 2010: 06-1). Adjacent foil defects are affected by the feeding and guiding mechanism of the sonotrode and improvements in those systems yield improved welds (Obielodan, Janaki Ram, Stucker, & Taggart, 2010: 06-7). Further, the increase in power available in UAM machines has substantially improved the welds produced.

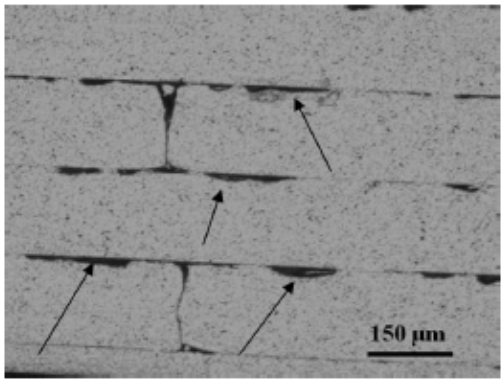

Figure 2. Interlayer Bond Defects (Obielodan, Janaki, Stucker, & Taggart, 2010: 6-2)

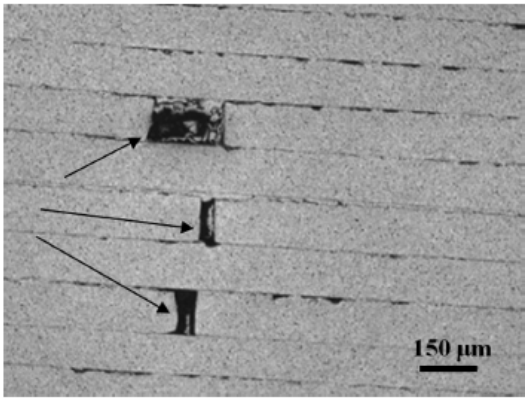

Figure 3. Adjacent Foil Bond Defects (Obielodan, Janaki, Stucker, & Taggart, 2010: 6-2)

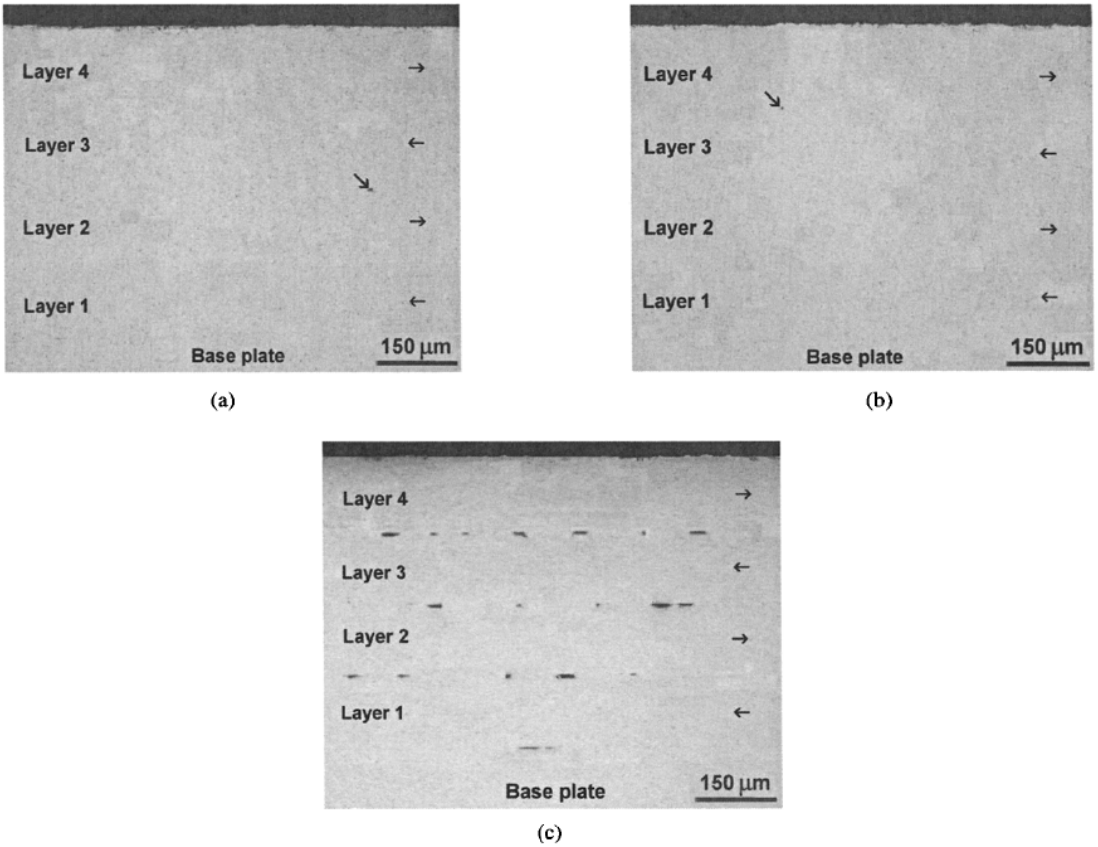

Figure 4. UAM deposits with intermediate surface machining, (a) welding speed: 28 mm/s, (b) welding speed: 36 mm/s, (c) welding speed: 40 mm/s (Janaki, Yang, & Stucker, 2006: 265)

Design Process

From conceptualization to application, the AM process consists of seven steps with design being critical to the success of the part. Figure 5 shows a process flow developed during the course of this research. These steps may be eliminated or modified depending on the AM process type, but the figure is a baseline framework for creating an AM product. This section reviews the various aspects of design in AM and suggests considerations for successful building using an AM system.

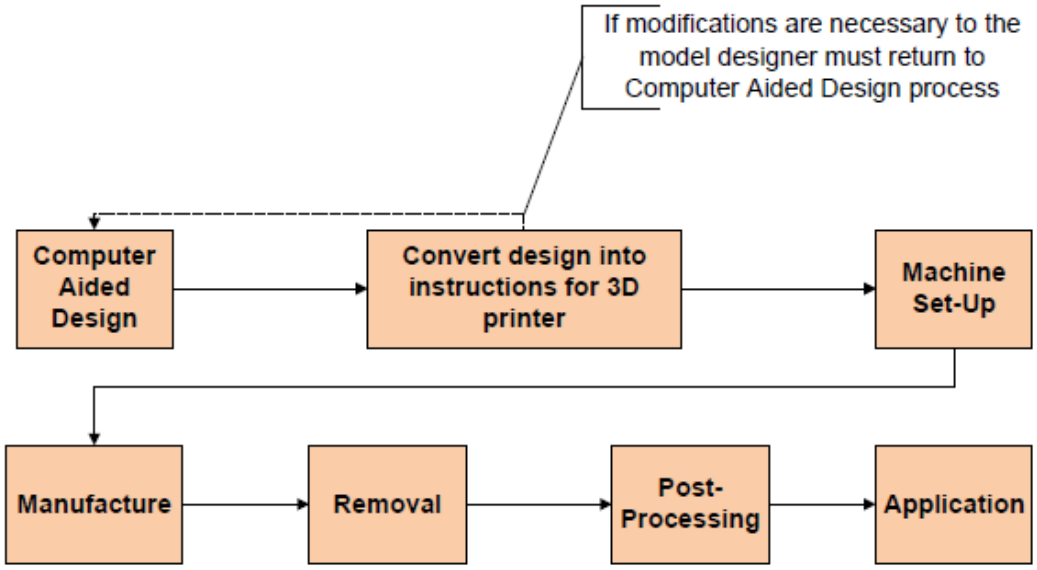

Figure 5. 3D Printing Process

Early Considerations

The first step is to have an idea. Usually, an idea derives from a requirement for a structure or component that would improve a system or artifact, and this requirement is not readily available through the traditional manufacturing stream. AM requires an adjustment in the mindset of engineers, designers, operators, and managers because of the

different manufacturing considerations in AM (Kuhn & Collier, 2014). AM excels at creating one of a kind, complex parts for inclusion into an existing machine (Kuhn & Collier, 2014). When undertaking the design process, the engineer should consider the printability, usability, and material selection up-front and throughout the design process.

Printability

The component's printability consists of rendering a model which that includes the fewest possible bridges, overhangs, and unsupported ends (Smyth, 2013: 7). These structures are put in place manually or by a design program to support the build while material the material cures. Reduction in the number of additional structures, such as bridging and overhangs is accomplished when designers ensure their component has an axis and orientation conducive to minimizing the additional construction. Many structures created through AM require support structures generated either by the designer or automatically through the machine programming (Smyth, 2013: 7). When a design requires supports, manual design is usually better than the program's automatically generated features (Kuhn & Collier, 2014). Supports should be designed for both easy removal after building and strong adherence to the printer build platform (Smyth, 2013: 7). Therefore, supports increase the complexity of the design, and printability of the part.

Every element built in an AM machine requires support from a layer beneath it. The machine's build platform, previously "built-up" layers, or designed support structures provide this support (Smyth, 2013: 8). As an example, consider the *T*-shape marked "A" in Figure 6. The free-hanging ends of the *T* cannot be printed without support. Every element of the build must be supported somehow the AM machine will construct support structures to build the free-hanging ends, but these structures will

require more material, build time, and post-process time (Smyth, 2013: 8). To incorporate printability a designer should consider the components in “B” or “C” which have no free-hanging ends and, therefore, will not require additional support scaffolding or other structures.

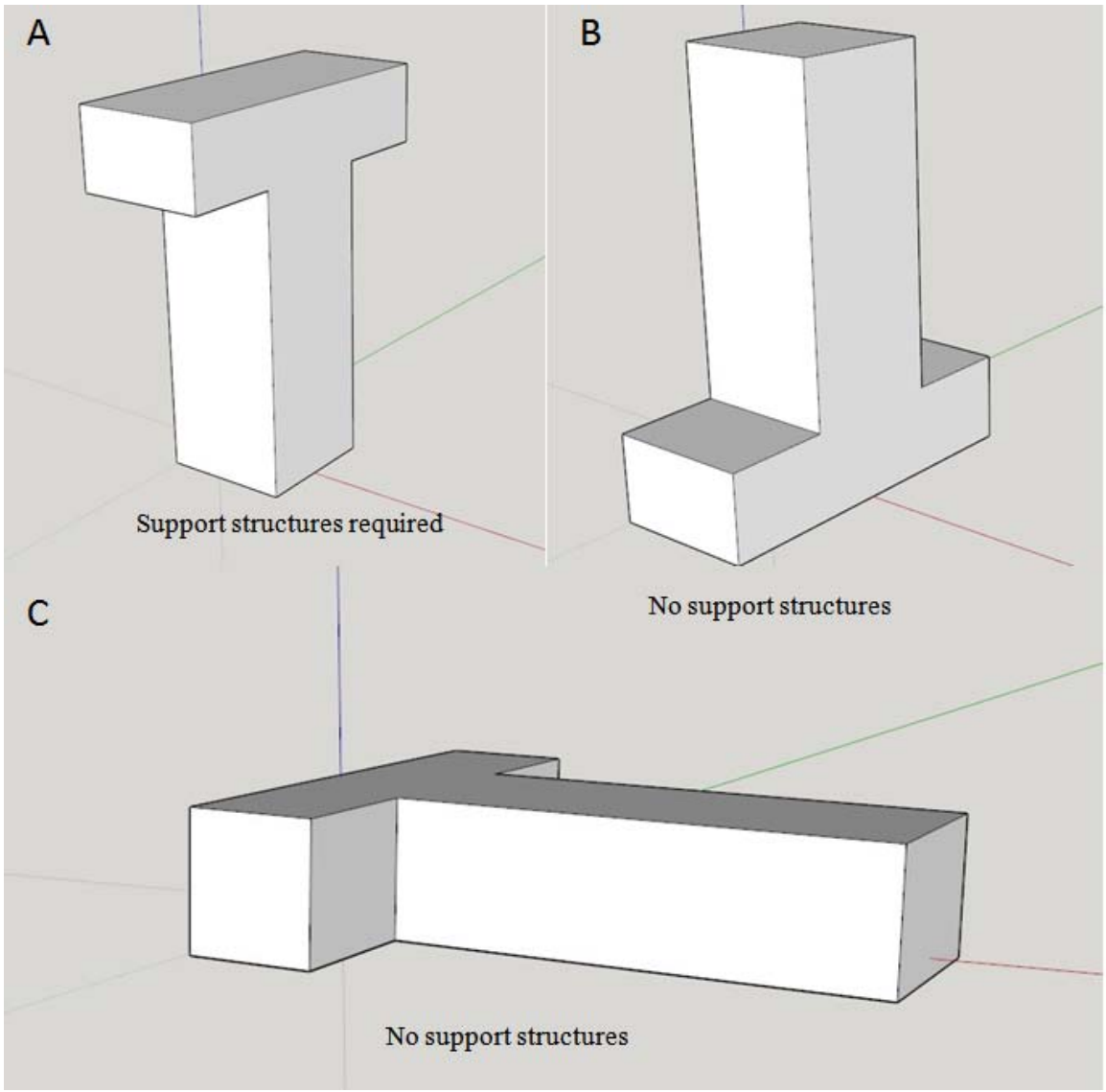

Figure 6. T-Section Examples (Smyth, 2013)

Usability

The next concept a designer should consider when undertaking in AM is usability. Usability addresses the suitability of the printed part to the purpose for which it was designed (Smyth, 2013: 9). Strength, shape, proportion, size, weight, and flexibility are examples of characteristics the finished object should meet to perform its function (Smyth, 2013: 9). Usability characteristics may necessitate changes to some of the designed parameters. The magnitude and direction of the load applied may affect how a component operates (Kuhn & Collier, 2014).

Material Selection

The third concept a designer should consider is what material is best suited for the build and what material is available to use. Typically, the choice of material is determined by the intended use of the object being built (Smyth, 2013: 11). However, the acceptable range for weight and size of the component available material, and environmental conditions may affect the printed component (Smyth, 2013: 10). Material selection also affects post-processing of components.

Converting 3D Models into Instructions

After a designer creates a 3D model, the next step is to convert the image into machine language that instructs the printer where and when to place build material. AM machines read instructions through G-Code which "slice" the 3D model into layers for construction (Weinhoffer, 2014: 45). Many developers have created distinct slicing programs (a list is tabulated in Appendix B). One example, and the slicing software used for this thesis is Slic3r™. Slic3r™ is commonly used program because it is free, open source, cross-platform, and customizable (Weinhoffer, 2014: 45). The slicing process

requires experimentation and iteration with machine settings to optimize the quality of the prints as no two machines are exactly the same (Weinhoffer, 2014: 45). Slic3r facilitates AM on different machines through its profile configuration which customizes unique settings based on the underlying firmware in use by the AM machine (Ranellucci, 2014).

Design for the AM Process: UAM

Understanding the technical capabilities of the AM machine in use is also critical to the design. The travel speed of the extruder, laser, or sonotrode; the amount of material used; bed adhesion of the build up; and the amount of cooling or other temperature variations are all technical characteristics of AM systems designers must consider (Smyth, 2013: 22). These technical aspects are unique to each machine type and can serve as either a capability or limitation. UAM machines, including the Fabrisonic machine employed in this research, Figure 7, have technical parameters which must be considered during design.

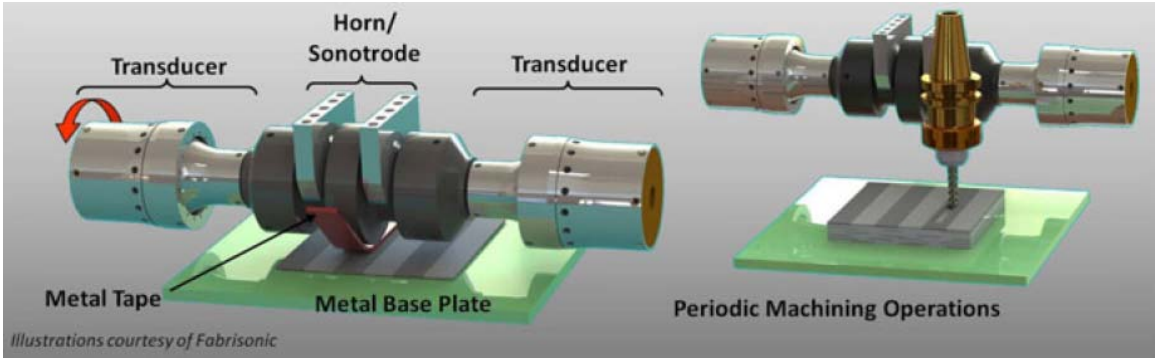

Figure 7. Schematic of Fabrisonic UAM Process (Wolcott, Hehr, & Dapino, 2014: 2056)

Some of these design considerations for UAM include temperature, power, normal force, and sonotrode travel speed. In fact, Wolcott, Hehr, and DaPino find that these factors have the most influence on the build (2014: 2056). The Fabrisonic 4200's sonotrode travel speed can range from 200 inches/minute to 1250 inches/minute (Wolcott, Hehr, & Dapino, 2014: 2058). The process uses a significant amount of material, not just in building the part but as excess along the edges from the initial transient region and overhang. The build area is held in place by vacuum suction at 25 inch Hg throughout a component's fabrication. The vacuum is necessary to reduce the movement of the build surface during the UAM process.

Summary

This chapter has reviewed AM technology and introduced a specific type of AM: UAM whereas, traditional manufacturing focuses on generating high volume products at the lowest cost, AM provides the ability to eliminate the manufacturing chain and produce complete components in one build. The build process comprises seven steps from design to production and requires a new approach to design. The new design approach has advantages but also significant limitations. The advantages included the ability to design and create unique structures and rapidly prototype while the disadvantages are high variance in quality, specifically interlayer bond defects and adjacent foil bond defects in UAM. This chapter closed with an overview into important AM design considerations concluding with design considerations for UAM.

III. Methodology

Chapter Overview

This chapter describes the methodology employed for the design, build, and test of the baseplate test section model. The details of data collection are described in addition to actions taken in the design process identified in chapter two. The objective of this research is to compare the strength of on ultrasonic additive manufacturing (UAM) produced component to that of the currently used cast baseplate. To conduct this study, non-destructive evaluation (NDE) is conducted on a UAM produced cube and the original A356.0 cast aluminum baseplate. The UAM cube is the failed build of the test specimen designed for this analysis. The data collected from NDE is compiled in Appendix E.

Part Selection

To find and select a component to design and build through UAM, the author took a fact-finding trip to Holloman Air Force Base, New Mexico, and met with members of the 49th Material Maintenance Squadron to learn which parts fail on expeditionary shelter equipment. Through interviews with group leaders and the equipment maintenance craftsman, three parts were identified as the best candidates for UAM in this area due to their frequency of failure and importance to the shelter system. The baseplate was chosen for this proof-of-concept because it facilitated a simple build, which was also convenient for strength testing. Components identified included the Universal Fabric Dome shelter baseplate (Figure 8), the LAMS joiner rod (Figure 9), and the Large Area

Maintenance Shelter (LAMS) baseplate (Figure 11). The LAMS baseplate was eventually selected as the experimental test section.

Figure 8. Universal Fabric Dome Shelter Baseplate

Figure 9. LAMS joiner rod

Part Design

The three-dimensional modeling of the LAMS baseplate began with measurement of the A356.0 original baseplate and using SketchUp™ to recreate the digital design of the baseplate. For the design grid reference system International Standards Organization (ISO) industrial automation systems and integration, numerical control of machines, coordinate system and motion nomenclature, 841: 2001 defines three principal axes labeled *X,Y,Z,* and three rotational axes labeled *A,B,C* as shown in Figure 10. A standard orientation is necessary for a UAM so the process and results can be repeated.

To gain advantage from the material properties of UAM the part was oriented in a manner to maximize strength to prevent the presumed failure mode of shear fracture. Design outputs of the entire LAMS baseplate and test sections are presented in Appendix C. Further design considerations include the printability, usability, and production

material, as discussed in chapter two. Since UAM involves building up layers on a rigid base, the base was incorporated for a sizable portion of the build in order to save machine time and improve quality.

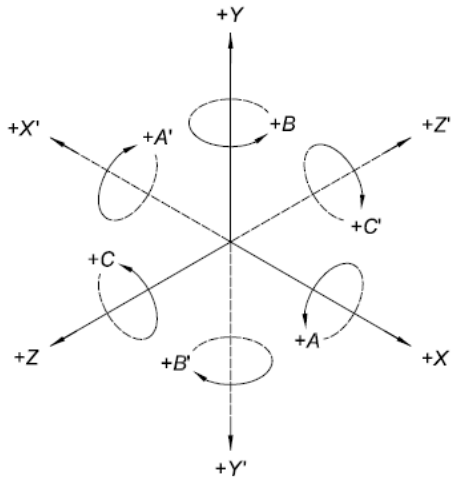

Figure 10. Right-Hand Coordinate System (International Standard, 2001: 6)

The entire baseplate shown in Figure 11 could not be printed with the available time and funding for this project. First, the baseplate would require extensive production time on the Fabrisonic machine which the Ohio State University (OSU) did not have available due to numerous projects and high demand of the machine. Second, funding was not available to print the entire baseplate. OSU provided a rough order of magnitude cost estimate for the entire plate to be $80K, far more than was allocated. To facilitate analysis, the baseplate was modeled as a test section displayed in Figure 17 of the appendices which could be loaded in the same manner as the original baseplate.

Figure 11. LAMS Baseplate

Usability of the test section is accounted for by ensuring the design contains the same dimensions and, therefore, may exhibit the same response stresses in a traditionally cast baseplate. If the designed test section can support the same load as the original cast baseplate specimen, the test validates the feasibility of UAM applications for CE expeditionary component productions. While a test section is not usable as part of a LAMS structure it can provide valuable proof-of-concept data and suggest the need for continued study.

Al-6061 is the chosen material based on suitable properties, availability of the material for the machine, and inherent mechanical advantages of Al-6061. A summary of the mechanical properties for both the original cast aluminum and the Al-6061 used to produce the test section is shown in Table 2. Nominal composition of the virgin Al-6061 used in the manufacture is shown in Table 3. Further technical specifications are displayed in Appendix D.

The properties are very similar, but Al-6061 may realize strength gains as a result of ultrasonic welding. Proper ultrasonic welding results in uniformity, reduction in void space, and optimal grain orientation within the component all contributing to increased strength (Janaki, Yang, & Stucker, 2006: 237). Another advantage is the high strength to weight ratio of Al-6061 material. This makes it potentially competitive for expeditionary environments. Finally, Al-6061 is standardized throughout most of the world as conventional welding grade aluminum and so replacement material will be higher in quality, due from regulation and experience of manufacture, anywhere globally.

Table 2. Summary Table A356.0 and Aluminum-6061 (MatWeb) (MatWeb)

	Material	
Property	A356.0	Aluminum-6061
Tensile Strength, Ultimate (psi)	34,000	45,000
Modulus of Elasticity	10,500	10,000
Shear Modulus (ksi)	3,950	3,770
Shear Strength (psi)	20,700	30,000

Table 3. Nominal Composition Properties of Al 6061 (MatWeb)

Property	Percentage in Al 6061
Mg	1.00%
Si	0.60%
Cu	0.28%
Cr	0.20%
Al	97.93%

Part Production

The test section shown in Figure 12 was produced on the Fabrisonic 4200™ at the Ohio State University (OSU) Smart Materials and Structures Lab using annealed, heat treated, H18, cold-worked Al-6061 due to the reasons discussed in the previous section.

In order to facilitate more rapid construction, a build plate was incorporated as half of the test section and the other half is built up strips of Al-6061 using UAM.

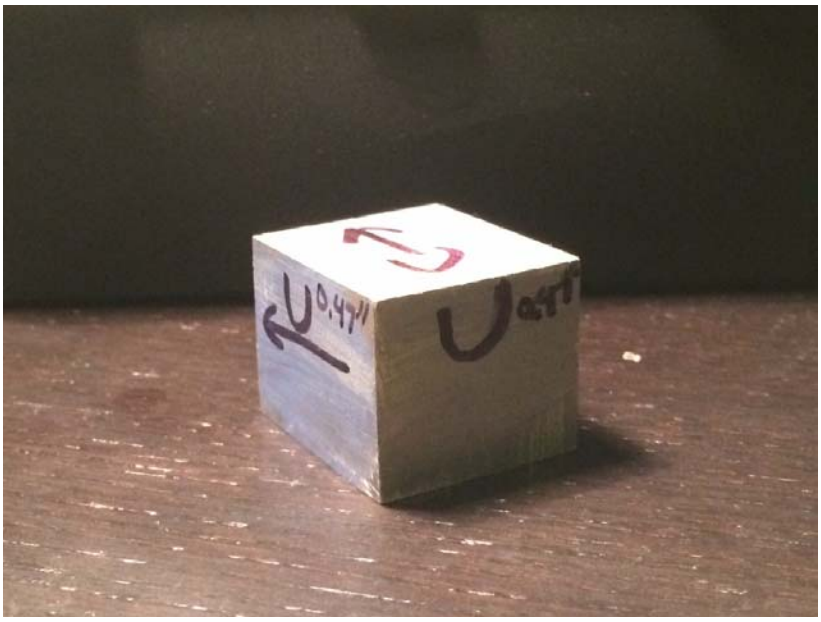

Figure 12. Block Produced at OSU (8 Nov 2014)

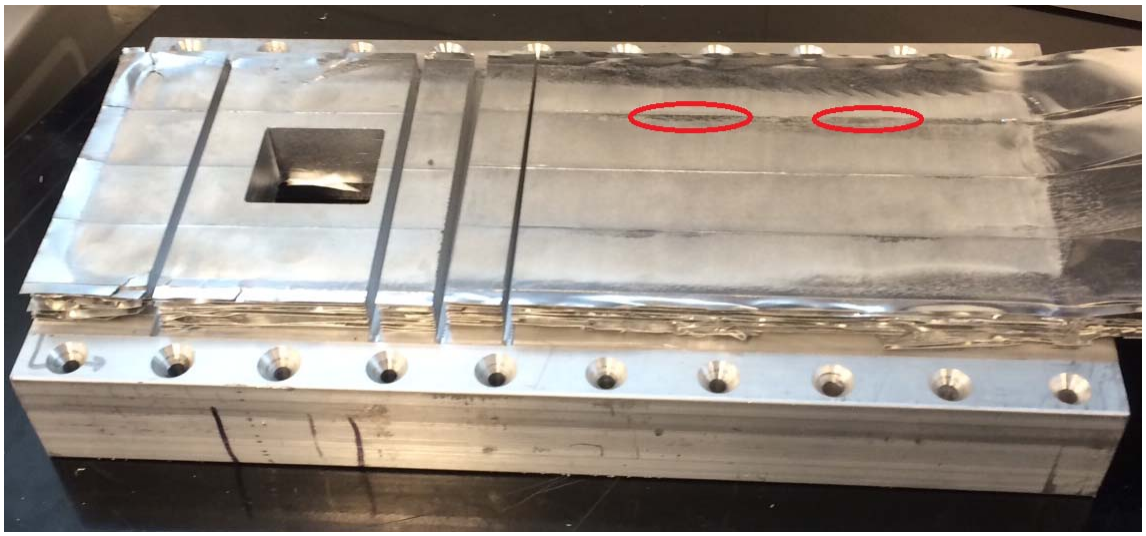

Figure 13. Overview of UAM Build at OSU, the red circles indicate areas of delamination (8 Nov 2014)

Machinists attempted to adjust the properties identified in the literature review: amplitude, normal force, weld speed, and layer surface roughness in an attempt to build the design shown in Figure 17. These process parameters are discussed below.

Amplitude

In operation, power to the UAM machine is input by the operator and maintained constant throughout operation (Wolcott, Hehr, & Dapino, 2014:2056). The value selected for the build was 33.6 μm. Amplitude refers to the height of the crest or trough of the frequency sound vibration (BBC, 2014). Increased power makes it possible to achieve welds without voids. The frequency at which the sonotrode vibrates is calibrated for the particular unit and remains constant during the process. The rationale for this level was past success in the lab with this parameter and its identification as a satisfactory build parameter for Al-6061 UAM welds (Wolcott, Hehr, & Dapino, 2014:2058).

Normal Force

Set to 5,000 N, this parameter acts to stabilize the piece under construction and allows power to be applied uniformly across the build suite. The machinist chose this setting because it allows the sonotrode to move at a consistent rate and reduce defects from the unwelded bits of "slag" shown in Figure 13 and circled in red.

Weld Speed

The weld speed for this build was set at 200 inches per minute based on previous satisfactory performance of the setting. Since the build experienced an interlayer failure the weld speed is a possible limiting factor in this study. With a reduced weld speed perhaps more energy may have transferred to the build layers resulting in stronger bonding.

Layer Surface Roughness

The operators at OSU textured the surface of the baseplate before the first layer of material was applied to create more deformation in the surface. The deformation would facilitate more consolidation in the weld. After the surface was textured, 20 layers of foil placement were welded between each layer of textured build-up.

Limitations

The resource limitation is a possible constraint to field application of the UAM technology. A large amount of time is required for a production on the scale of the LAMS baseplate. Time restraints are addressed in the Part Design section of this chapter.

Due to production problems, the actual product produced during this research is an aluminum block 1.252 inches long, 1.0695 inches wide, and 0.9345 inches high as shown in Figure 12. In order to achieve this, welding was performed on a baseplate with dimensions 11 inches long, 6 inches wide, and 1.5 inches high. Adjacent strip welding shown in Figure 13 was used to increase the strength of the test specimen. The strips were staggered to avoid consecutive seam placement which would theoretically improve bond strength and as a result overall part quality. If the strips were placed directly on top of one another crack propagation could occur much more readily through the build. During the build process delamination was observed along the *z*-axis after approximately 0.4345 inches of material deposit.

Failure Modes

The craftsman at Holloman AFB reported two failure modes for the LAMS baseplate. A structural member's failure mode depends on several factors including material type, load configuration, load rate, and environmental conditions (Riley, Sturges, & Morris, 2002: 146). Interviews about failure conditions conducted during an on-site visit with the 49 MMS craftsman identified two principle failure modes the baseplates display: the baseplates fail in a shear direction, usually when the assembled LAMS is subjected to high wind loads; they also fail from normal wear and tear during assembly and disassembly operations. Both failure modes typically result in complete separation of the baseplate material as shown in Figure 14, which is representative of the failures encountered in the field and what actually occurred. Because all the failures described resulted in complete separation of the baseplate material, this information implies that failure modes of the LAMS baseplate may be categorized as failure by fracture (Riley, Sturges, & Morris, 2002:146).

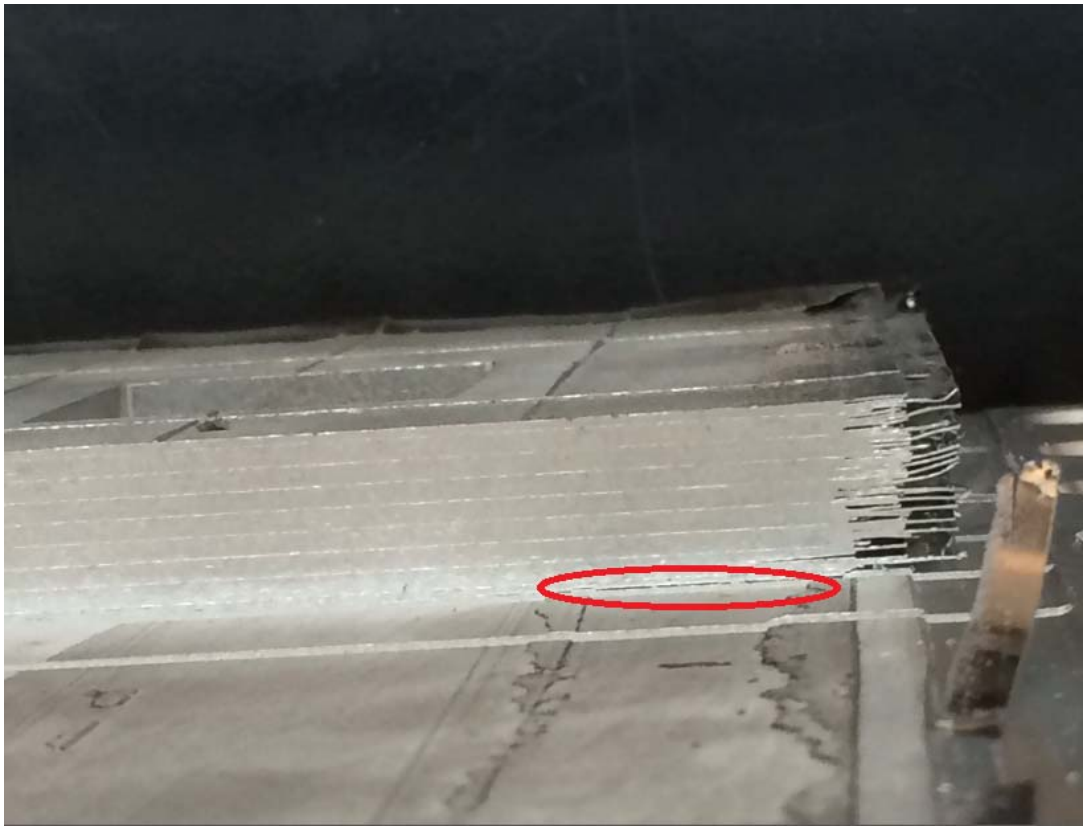

Figure 14. Observed interlayer failure (Nov 2014)

Non-Destructive Evaluation

Non-destructive evaluation (NDE) is used to determine the ratio of welds which contain anomalies. Two types of NDE were performed on the test specimen and cast A356.0 baseplate section: ultrasonic inspection (UI) and computed tomography (CT). The Air Force Research Lab (AFRL) conducted both NDE tests on the UAM produced test specimen and the original cast section. The results of the NDE are included in Appendix E. Ultimately, these anomalies will affect the structural performance of a component constructed through UAM. These tests provide information about the quality of the weld bonding throughout the specimens. An anomaly may include any aberration

from a consistent build area such as debris in between layers and not fully bonded layers. From this data, performance information can be inferred. The images generated through the UI are also scanned using the Python software package to calculate a weld quality ratio for the components. The equation for weld quality is presented below:

$$Weld\ Quality = \frac{Anomalies\ Detected}{Total\ Build\ Area}$$

Summary

This chapter described the methodology used to design, construct, and evaluate a UAM produced LAMS baseplate test section. It detailed the composition of the build material and the factors which are taken into account when designing a piece for the UAM process. It also introduced the NDE methods used to evaluate the test section versus a representative piece of the actual LAMS baseplate.

IV. Analysis and Results

Chapter Overview

This chapter discusses the results of the test section production and the evaluation of its strength properties. The NDE technique selected for this analysis was Ultrasonic Immersion (UI). UI analysis provides three output scans: A-scan, B-scan, and C-scan as shown Figure 18. The A-scan displays the amplitude of the anomaly in the block as tested. Anomalies could be caused by voids, porosity, or lack of fusion and they are indicated in Figure 15. The C-scan combines the amplitude detection in the A-scan with the depth the probe observes the anomaly to provide a visual representation of "good" welds. The C-scans were analyzed in Python to determine a weld quality percentage to compare with the assumed quality of the cast aluminum Large Area Maintenance Shelter (LAMS) baseplate. Based on this proof of concept, ultrasonic additive manufacturing (UAM) was unable to produce a usable LAMS baseplate with adequate physical properties at this time.

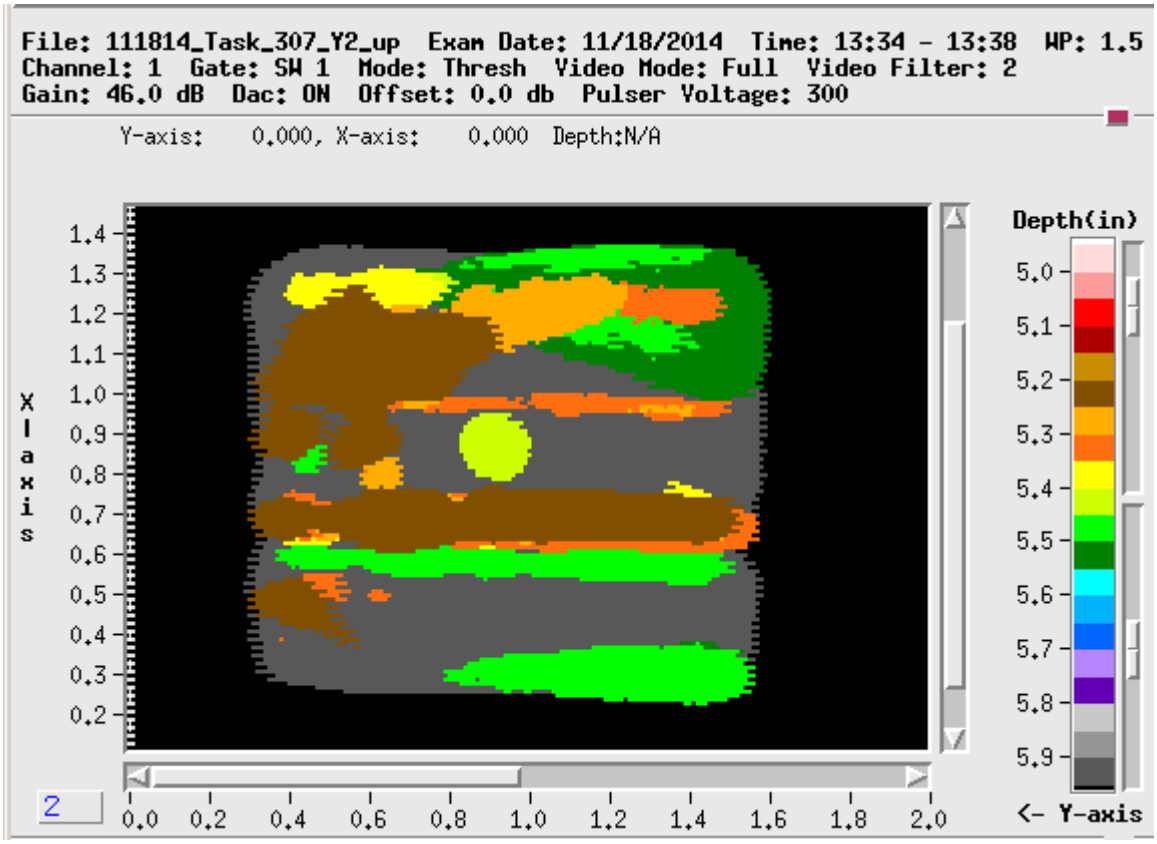

Figure 15. C-Scan Output

Investigative Questions Answered

The research question sought to compare whether a LAMS baseplate test section constructed with UAM was at least as robust as a traditionally procured baseplate. To that end, this proof-of-concept study demonstrated it is not possible to construct a LAMS baseplate both from a structural standpoint and a practical machine use perspective. The resulting specimen had numerous anomalies across the entire build area, the percentage of anomalies detected versus the "good" weld is presented in Table 4. The Fabrisonic was unable to replicate a LAMS baseplate or even a scaled model. Additionally, the unit

cost was high, especially considering the constructed test section accounted for only 7% of the desired LAMS baseplate dimensions.

Table 4. Weld Quality Percentages

View Direction	Good Weld	Defects
x	91.50%	8.50%
y	40.90%	59.10%
z	77.10%	22.90%

A weld is considered "good" if it is free from anomalies at the prescribed detection threshold of 25% and a gain setting of six decibels. The machine is set up to the specifications of a manual scan which uses a higher amount of gain which makes it easier to see defects. This detection threshold is used for objects where very little noise exists in the good areas. Consequently it allows for detection of the most defects in the specimen (Laufersweiler, 2014). The 25% setting is consistent with established procedures used for research specimens which attempt to detect as many anomalies as possible (Laufersweiler, 2014). These detections can be used to predict how the specimen may fail when subjected to destructive evaluation.

In Table 4 and Figure 20, the top down (*y*-axis) view of the block shows a substantial number of anomalies which is indicative of a very poor weld and interlayer failure. Poor interlayer bonding would indicate a high likelihood of delamination or fracture in the component under load (Obielodan, Janaki, Stucker, & Taggart, 2010: 06-1). Delamination occurred during the build process without any load application to the build surface other than the sonotrode building up the layers.

From these results, it would appear that UAM is poorly suited to constructing load bearing LAMS baspeplates at this time. Currently, UAM is better suited for other kinds of projects particularly smart materials, so further research may focus on smart material applications to expeditionary operations.

Cost

The total cost of production for the test specimen is incomplete due to the fact a complete baseplate was not actually produced in this research. Recall from Figure 12 that only a small portion of the LAMS baseplate was reproduced for testing. Regardless, cost information obtained during this research are included in Table 5. Approximately 60% of the cost arose from the machine time at OSU. This included approximately 20 hours of work on the Fabrisonic and two graduate assistants. Part identification is also a significant cost since it requires the researcher to physically visit the location of potential components. Design time is based on the equivalent hourly pay rate for an O-3 Captain calculated using the Office of Personnel Management (OPM) Fact Sheet on equivalent annual compensation (U.S. Office of Personnel Management, 2015). The amount of time spent on the test section design is approximately five hours.

Table 5. Cost Data for Test Specimen Production

Line Item	Cost
TDY to Holloman AFB, NM	$1,716.22
TDY to America Makes training Youngstown, OH	$2,886.98
Material and Machine Time at OSU	$7,000.00
Design Time	$172.00
Total per unit cost	$11,775.20

Summary

UAM was unable to produce a complete test specimen for this study with the machine available at OSU. Delamination was observed during the build after the first approximately 0.4345 inches of material placement which resulted in an inability to place further layers. The sample was analyzed with UI and found to be poor quality due to the significant amount of anomalies across all build surfaces. Based on this sample, in this configuration, UAM is not ready for application in CE expeditionary operations due to an inability to produce the actual size component and numerous anomalies throughout the build.

V. Conclusions and Recommendations

Chapter Overview

This research examined whether a Large Area Maintenance Shelter (LAMS) baseplate produced through ultrasonic additive manufacturing (UAM) is at least as robust as a traditionally procured cast baseplate. To accomplish this objective, first a high failure component on the Civil Engineer (CE) Base Expeditionary Airfield Resources (BEAR) kits was identified, next the identified part was reproduced for UAM using Computer Aided Design (CAD) software, constructed at Ohio State University (OSU), and evaluated by the Air Force Research Laboratory (AFRL). Further research areas including a Taguchi design of experiments (DOE), and other possible applications are also presented.

Conclusions of Research

The research found that while UAM is an exciting technology, and may eventually provide many valuable capabilities, it is not ready for structural applications in a CE expeditionary environment. This conclusion was based on a single proof-of concept experiment conducted for this research. However, technology continues to change and improve and perhaps future iterations of UAM machines may facilitate better construction in the future. Therefore, the research into UAM and its applications should not be abandoned.

Significance of Research

This research is significant because it attempts to apply a new technology to expeditionary CE applications. At this time, the technology is not ready to provide usable components of suitable strength. Over time, the capabilities of UAM may increase to the point where they may be employed effectively in expeditionary applications.

Based on the findings of this research, the Air Force Civil Engineering career field, in the short term, should look to other techniques in additive manufacturing (AM) to explore and invest. Long term actions of the career field should be to observe and watch UAM developments until structurally sound parts can be produced.

Recommendations for Action

The results of this research indicated UAM is not able to produce and support structural loads which are required in CE expeditionary environments. Since this was only a proof-of-concept study, further research is necessary to uncover improvements in the process, or find the proper application of UAM in CE operations.

Recommendations for Future Research

Potential follow-on research into UAM may include Taguchi design of experiments (DOE) to uncover the effect the identified process parameters have on the build. A DOE, especially a Taguchi method, focuses on evaluating main effects selected parameters have on an observed response variable, and the interactions between factors as a secondary consideration (Frigon & Matthews, 1997: 182). The Taguchi method is tpically developoped in eight steps listed on the next page (Frigon & Matthews, 1997: 182).

1. Identify an element of the system design for analysis
2. Perform a cause-and-effect analysis
3. Select treatments, levels, and values
4. Determine how experimantal results will be expressed
5. Select a designed experiment
6. Conduct the experiment
7. Perform data analysis
8. Graph the results (Frigon & Matthews, 1997: 182)

Using this methodology, future researchers could analyze the effects the different parameters of UAM have on the build. The previously identified factors: oscilation amplitude, weld speed, normal force, and layer surface roughness could be analyzed at different settings. Other parameters to consider include temperature, adjacent foil overlap, different materials, foil orientation, and foil thickness. The parameters are presented in Table 6 to simplify the orthogonal array presented later. The values selected are a derived from anecdotal experience in the build process in this research and previously selected values chosen by Wolcott et al (2014: 2058).

Table 6. Taguchi Parameter Coding

Parameter Code	**Parameter Name**	**Level (1)**	**Level (2)**	**Level (3)**
A	Amplitude	28.23 µm	30.47 µm	30.76 µm
B	Weld speed	200 in/min	175 in/min	150 in/min
C	Normal force	4 kN	5 kN	6 kN
D	Roughness	Every 25 layers	Every 20 layers	Every 15 layers
E	Temperature	22.2°	93.3°	121.1°C
F	Overlap	¼ distance to center	⅓ distance to center	½ distance to center
G	Materials	1.5 mm	2.0 mm	2.5 mm
H	Orientation	All parallel	Rotate 45°	Rotate 90°
I	Thickness	.006 in	.008 in	.010 in

Using these parameters, and following a similar process to the study conducted by Wolcott, Hehr, and Dapino, a L27 Taguchi matrix design may be developed to investigate the main effects these parameters have on build construction (Fraley, Oom, Terrien, & Zalewski, 2007). An example of such a scenario is presented in Table 7. At this time the machine at Ohio State University may not be configured to change all the parameters identified, but an opportunity may arise to accomplish the test through coordination of existing projects in the production queue.

Table 7. L27 Taguchi Matrix, (Fraley, Oom, Terrien, & Zalewski, 2007)

	Parameters								
Run Number	**A**	**B**	**C**	**D**	**E**	**F**	**G**	**H**	**I**
1	1	1	1	1	1	1	1	1	1
2	1	1	1	1	2	2	2	2	2
3	1	1	1	1	3	3	3	3	3
4	1	2	2	2	1	1	1	2	2
5	1	2	2	2	2	2	2	3	3
6	1	2	2	2	3	3	3	1	1
7	1	3	3	3	1	1	1	3	3
8	1	3	3	3	2	2	2	1	1
9	1	3	3	3	3	3	3	2	2
10	2	1	2	3	1	2	3	1	2
11	2	1	2	3	2	3	1	2	3
12	2	1	2	3	3	1	2	3	1
13	2	2	3	1	1	2	3	2	3
14	2	2	3	1	2	3	1	3	1
15	2	2	3	1	3	1	2	1	2
16	2	3	1	2	1	2	3	3	1
17	2	3	1	2	2	3	1	1	2
18	2	3	1	2	3	1	2	2	3
19	3	1	3	2	1	3	2	1	3
20	3	1	3	2	2	1	3	2	1
21	3	1	3	2	3	2	1	3	2
22	3	2	1	3	1	3	2	2	2
23	3	2	1	3	2	1	3	3	3
24	3	2	1	3	3	2	1	1	1
25	3	3	2	1	1	3	2	3	1
26	3	3	2	1	2	1	3	1	2
27	3	3	2	1	3	2	1	2	3

An L27 orthogonal array requires a high volume of tests. Careful selection of design parameters in future research are required to isolate specific effects on the build produced. From the results in this research, it appears weld speed and amplitude had a significant effect. Temperature and material thickness are also valid tests future researchers may consider since there is already some research into the effects of weld speed and amplitude.

Future research in this area may include the exploration of embedded sensors and manufacture of smaller replacement parts which do not have significant structural load requirements. For example, CE Explosive Ordinance Disposal (EOD) technicians often have a requirement for unique pieces and adaptors which an AM capability could rapidly prototype in the field. The future research does not have to focus exclusively on UAM, it might be possible to use one of the other techniques reviewed in chapter two such as fused deposition modeling or selective laser sintering.

The AF could possibly research using AM to design and build customized tools and jigs (Kuhn & Collier, 2014). The ability to prototype a tool which may otherwise have to be ordered and machined could improve overall infrastructure maintenance as well as save time and money. AM combined with existing equipment and tools may also be a useful application of the technology in the future.

In addition to possible EOD use, AM technology may be applicable to channelized components. Channelized components may be used in water pumps for heat exchange. Instead of ordering expensive replacement parts for outdated systems, or committing resources to extensive repair projects, components could be fabricated

through UAM to replace failed heat exchanging parts. These components would extend the service life of AF infrastructure assets.

As discussed in a potential Taguchi analysis, offsetting the angles of foil orientation could yield improvements in build quality as shown in Figure 16. The current UAM machine could be configured to deposit sheets of material laminated together by changing the orientation of the foils (Dowling, 2013). Bond strength could be improved through the incorporation of such a technique; however the machine time would increase significantly with the increased complexity of the build. Changes in the orientation may further inhibit crack propagation which could assist in preventing the fracture (delamination) failure mode observed during construction.

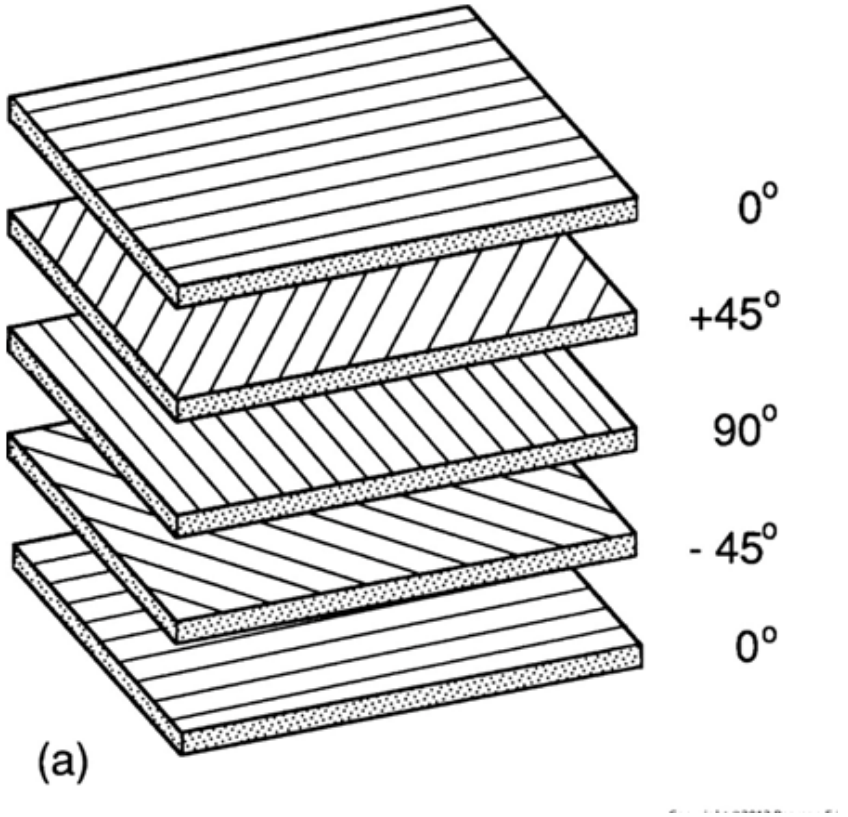

Figure 16. Offsetting Grain Orientation, (Dowling, 2013)

Summary

Ultimately the study found that UAM technology is not ready for CE expeditionary applications to produce a LAMS baseplate at this time. This thesis began with the goal of manufacturing a LAMS baseplate through UAM to compare with the traditionally cast baseplate. The design of a LAMS baseplate was replicated and UAM production of a representative test section was attempted. During the build, delamination was observed which prevented any further layer build up. After inspection the results indicated there was significant interlayer bonding defects in the piece as it was designed and manufactured. Additionally, the comparison between the empirically derived percentages from the scans compared to the assumed cast baseplate quality indicates UAM is not able to consistently produce a structure for use in the LAMS kit. As the technology continues to improve, it is possible it may develop to a point where it can produce welds of sufficient strength quality to support expeditionary structural applications.

Appendix A: 3D CAD Software

Table 8. 3D CAD software summary (Weinhoffer, 2014: 197-199)

Software	Developer	Description
Solidworks	Dassault Systemes	Professional grade, comprehensive modeling package, typically used by design companies and large institutions
AutoCAD	Autodesk	Professional grade, comprehensive modeling package, typically used by design companies and large institutions
SketchUp	Trimble	Free, easy to use software for generating 3D models, requires an add-on to convert files to .stl format
123D Design	Autodesk	Free, easy to use interface, allows designer to export designs as .stl files or send them to pre-identified fabrication companies
TinkerCAD	Autodesk	Web-based model generating program, interface runs directly in browser, files can be exported as .stl or sent to fabrication companies
OpenSCAD	Marius Kintel, Clifford Wolf	Programs 3D models using lines of code as opposed to drawing with a mouse and graphical interface, can export files as .stl

Appendix B: Slicer Software

Table 9. Slicer software summary (Weinhoffer, 2014: 200)

Software	Developer	Description
Slic3r	Slic3r	Wide-spread, free, open source slicing software which allows configuration for multiple machines facilitating faster production times
CuraEngine	Ultimaker	Open source software developed for Ultimaker™ printers, usable by other G-code based printers, slices automatically each time you make change to your model or settings
MakerBot Slicer	MakerBot	Software developed for MakerBot printers, fast and accurate part of the MakerBot Desktop Solutions package
Skeinforge	RepRap	Python based package in use for many years, becoing less popular with the rise in more accessable open source packages

Appendix C: CAD Design Outputs

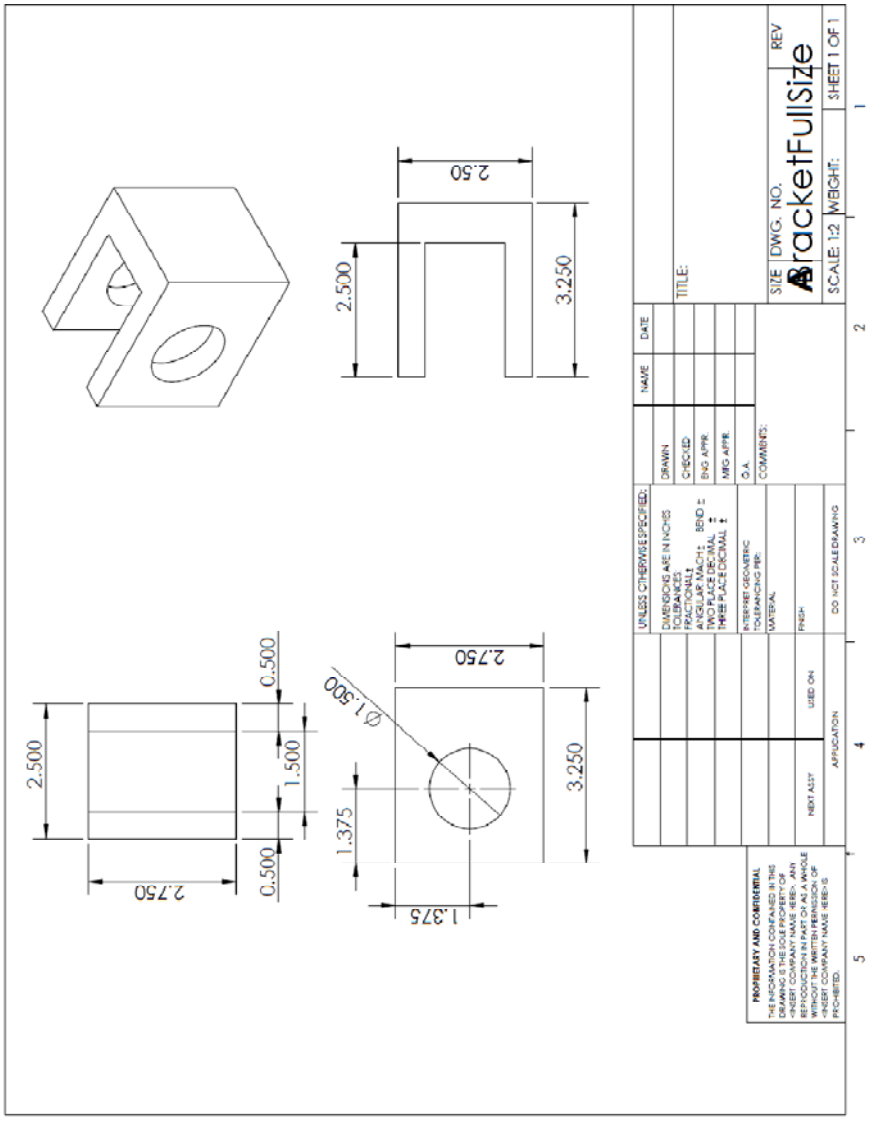

Figure 17. LAMS baseplate test section design

Appendix D: Material Specifications

Table 10. Aluminum 6061-T6 Properties, (MatWeb)

Aluminum 6061-T6; 6061-T651		
Physical Properties	**Metric**	**English**
Density	2.70 g/cc	0.0975 lb/in^3
Mechanical Properties		
Hardness, Brinell	95	95
Hardness, Knoop	120	120
Hardness, Rockwell A	40	40
Hardness, Rockwell B	60	60
Hardness, Vickers	107	107
Tensile Strength, Ultimate	310 MPa	45000 psi
Tensile Strength, Yield	276 MPa	40000 psi
Elongation at Break	0.17	0.17
Modulus of Elasticity	68.9 GPa	10000 ksi
Notched Tensile Strength	324 MPa	47000 psi
Ultimate Bearing Strength	607 MPa	88000 psi
Bearing Yield Strength	386 MPa	56000 psi
Poissons Ratio	0.33	0.33
Fatigue Strength	96.5 MPa	14000 psi
Fracture Toughness	29.0 MPa½	26.4 ksi-in½
Machinability	0.5	0.5
Shear Modulus	26.0 GPa	3770 ksi
Shear Strength	207 MPa	30000 psi
Electrical Properties	Metric	English
Electrical Resistivity	0.00000399 ohm-cm	0.00000399 ohm-cm
Thermal Properties		
CTE, linear	23.6 µm/m-°C	13.1 µin/in-°F
	Temperature 20.0 - 100°C	Temperature 68.0 - 212°F
Specific Heat Capacity	0.896 J/g-°C	0.214 BTU/lb-°F
Thermal Conductivity	167 W/m-K	1160 BTU-in/hr-ft²-°F
Melting Point	582 - 651.7°C	1080 - 1205°F
Solidus	582°C	1080°F
Liquidus	651.7°C	1205°F
Processing Properties		
Solution Temperature	529°C	985°F
Aging Temperature	160°C	320°F
	177°C	350°F
Component Elements Properties		
Aluminum, Al	95.8 - 98.6 %	95.8 - 98.6 %
Chromium, Cr	0.04 - 0.35 %	0.04 - 0.35 %
Copper, Cu	0.15 - 0.40 %	0.15 - 0.40 %
Iron, Fe	<= 0.70 %	<= 0.70 %
Magnesium, Mg	0.80 - 1.2 %	0.80 - 1.2 %
Manganese, Mn	<= 0.15 %	<= 0.15 %
Other, each	<= 0.05 %	<= 0.05 %
Other, total	<= 0.15 %	<= 0.15 %
Silicon, Si	0.40 - 0.80 %	0.40 - 0.80 %
Titanium, Ti	<= 0.15 %	<= 0.15 %
Zinc, Zn	<= 0.25 %	<= 0.25 %

Table 11. A356.0 Properties, (MatWeb)

Aluminum A356.0-T6, Sand Cast		
Physical Properties	**Metric**	**English**
Density	2.67 g/cc	0.0965 lb/in^3
Mechanical Properties		
Hardness, Brinell	70 - 105	70 - 105
Hardness, Knoop	112	112
Hardness, Rockwell A	37	37
Hardness, Rockwell B	55	55
Hardness, Vickers	99	99
Tensile Strength, Ultimate	>= 234 MPa	>= 34000 psi
Tensile Strength, Yield	>= 165 MPa	>= 24000 psi
Elongation at Break	>= 3.5 %	>= 3.5 %
Modulus of Elasticity	72.4 GPa	10500 ksi
Poissons Ratio	0.33	0.33
Machinability	0.5	0.5
Shear Modulus	27.2 GPa	3950 ksi
Shear Strength	143 MPa	20700 psi
Electrical Properties		
Electrical Resistivity	0.00000440 ohm-cm	0.00000440 ohm-cm
Thermal Properties		
Heat of Fusion	389 J/g	167 BTU/lb
CTE, linear	21.4 µm/m-°C	11.9 µin/in-°F
	Temperature 20.0 - 100°C	Temperature 68.0 - 212°F
	23.2 µm/m-°C	12.9 µin/in-°F
	Temperature 20.0 - 300 °C	Temperature 68.0 - 572°F
Specific Heat Capacity	0.963 J/g-°C	0.230 BTU/lb-°F
Thermal Conductivity	151 W/m-K	1050 BTU-in/hr-ft^2-°F
Melting Point	557 - 613°C	1030 - 1140°F
Solidus	557°C	1030°F
Liquidus	613°C	1140°F
Processing Properties		
Melt Temperature	677 - 816°C	1250 - 1500°F
Solution Temperature	535 - 540.6°C	995 - 1005°F
Aging Temperature	152 - 157°C	305 - 315°F
Casting Temperature	677 - 788 °C	1250 - 1450°F
Component Elements Properties		
Aluminum, Al	91.1 - 93.3 %	91.1 - 93.3 %
Copper, Cu	<= 0.20 %	<= 0.20 %
Iron, Fe	<= 0.20 %	<= 0.20 %
Magnesium, Mg	0.25 - 0.45 %	0.25 - 0.45 %
Manganese, Mn	<= 0.10 %	<= 0.10 %
Other, each	<= 0.05 %	<= 0.05 %
Other, total	<= 0.15 %	<= 0.15 %
Silicon, Si	6.5 - 7.5 %	6.5 - 7.5 %
Titanium, Ti	<= 0.20 %	<= 0.20 %
Zinc, Zn	<= 0.10 %	<= 0.10 %

Appendix E: UI Outputs

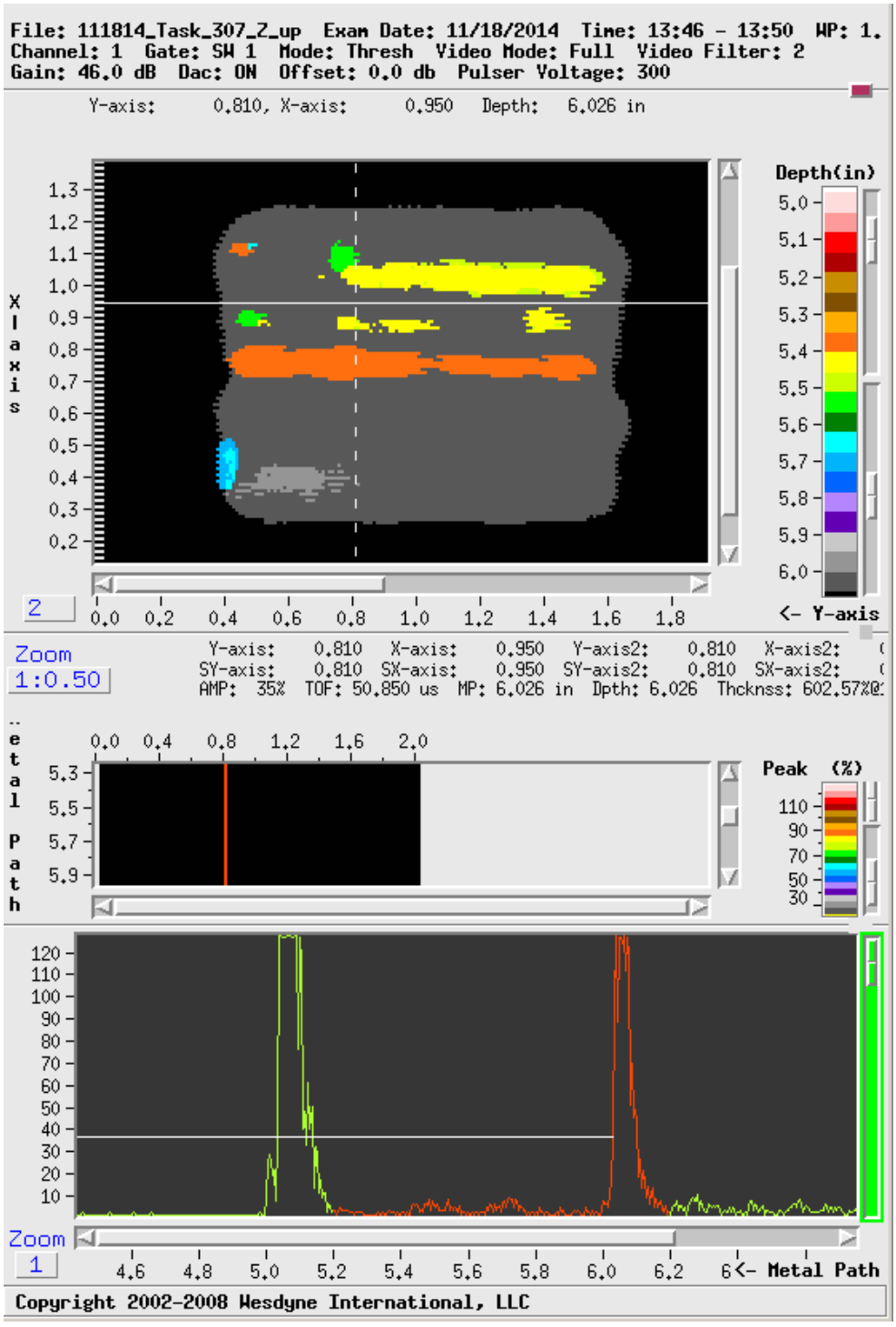

Figure 18. C-Scan output *x*-axis view, represents amplitude at weld location with no detectable anomaly indications

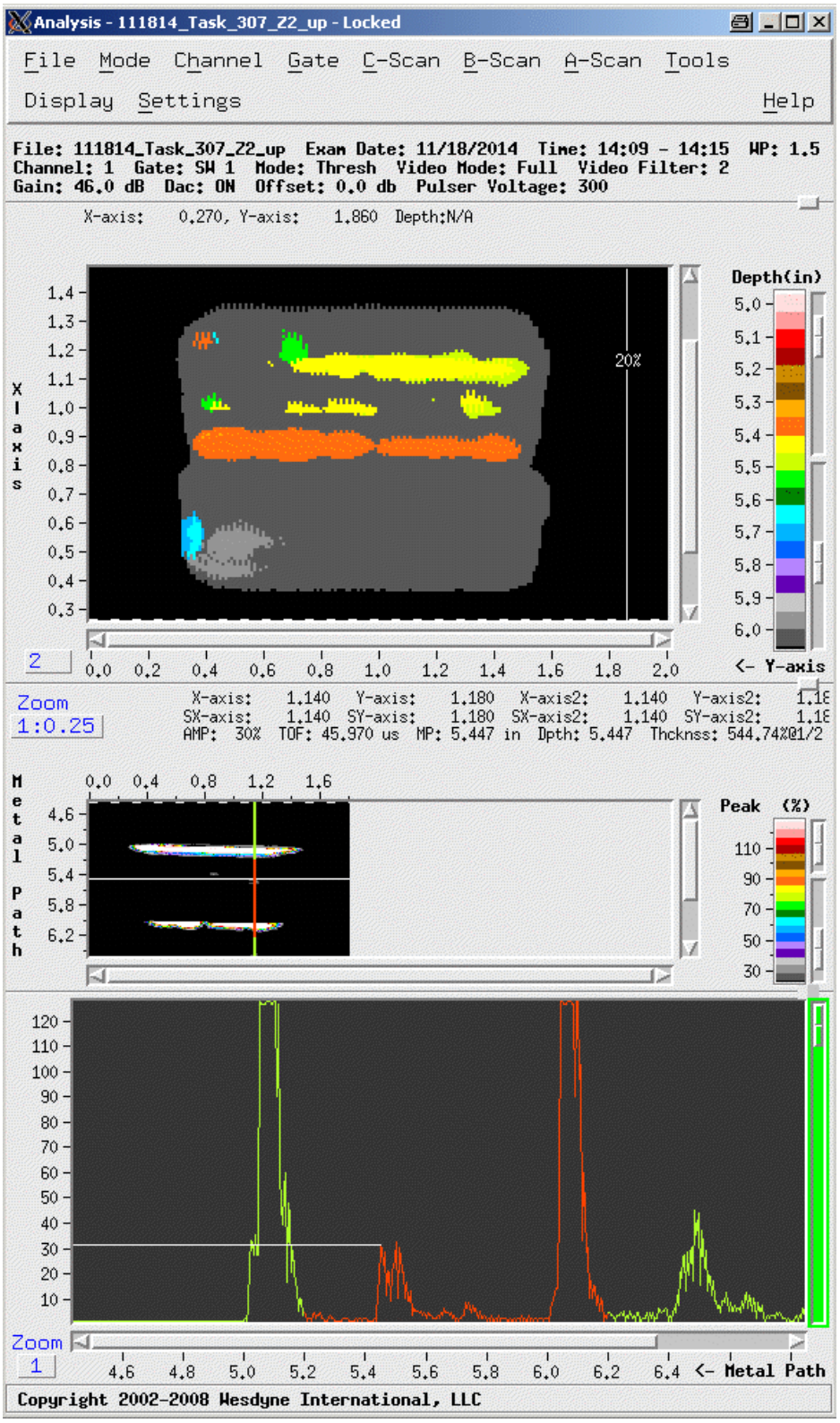

Figure 19. C-scan output *x*-axis view, representing detection at approximately .4 inches

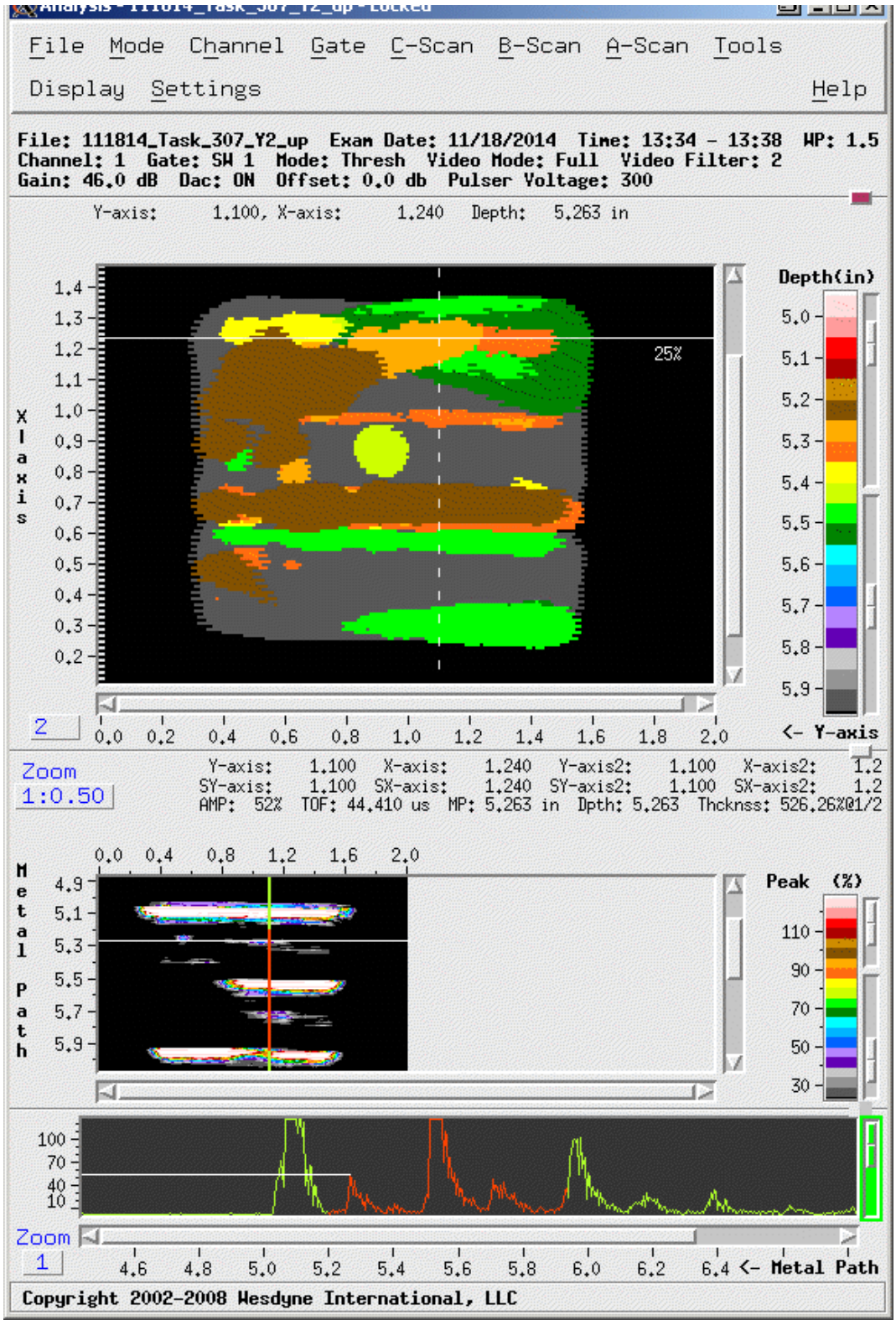

Figure 20. C-Scan output *y*-axis view, represents numerous anomaly detections

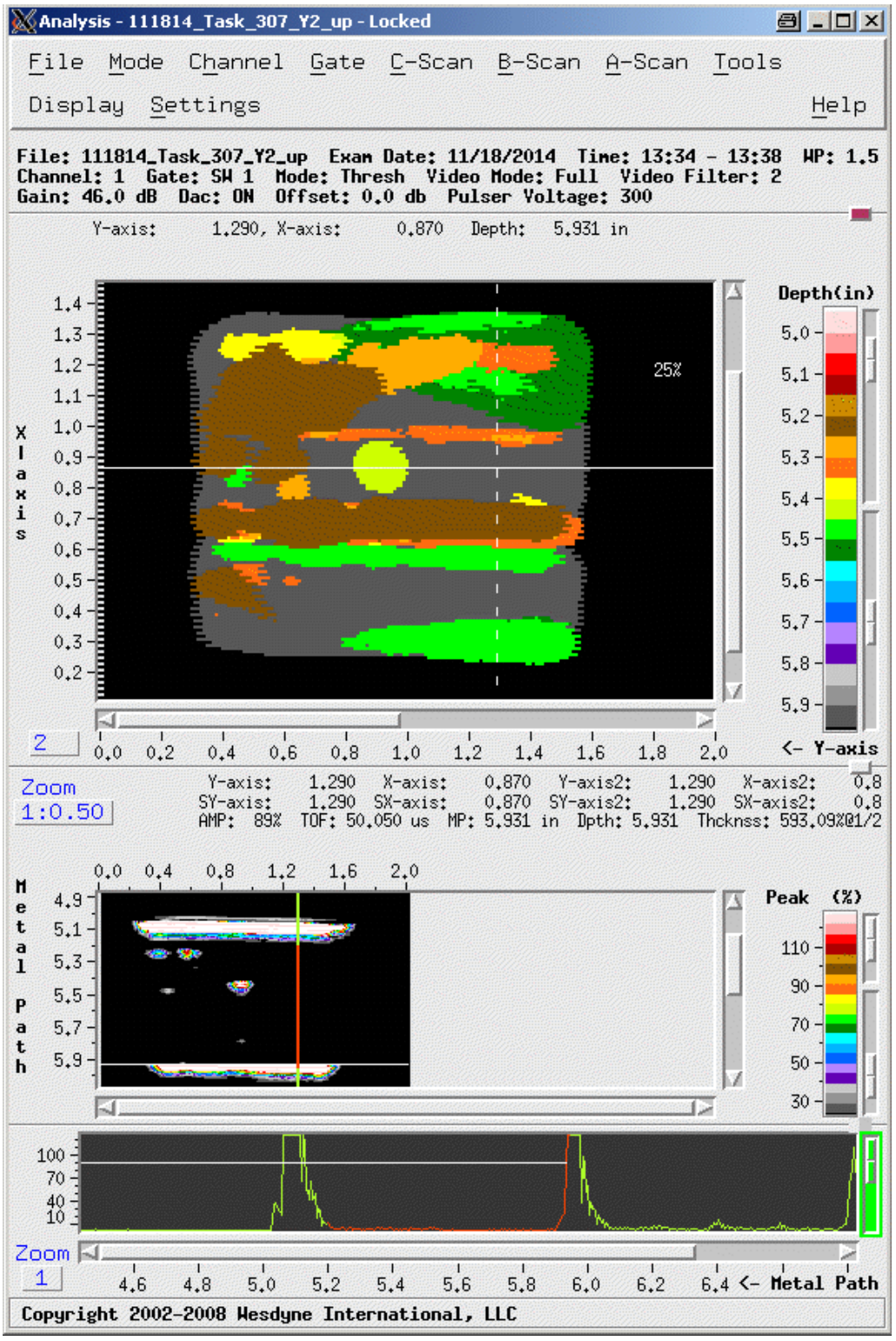

Figure 21. C-Scan output *y*-axis view, represents numerous anomaly detections with selector pointed at an anomaly free weld location

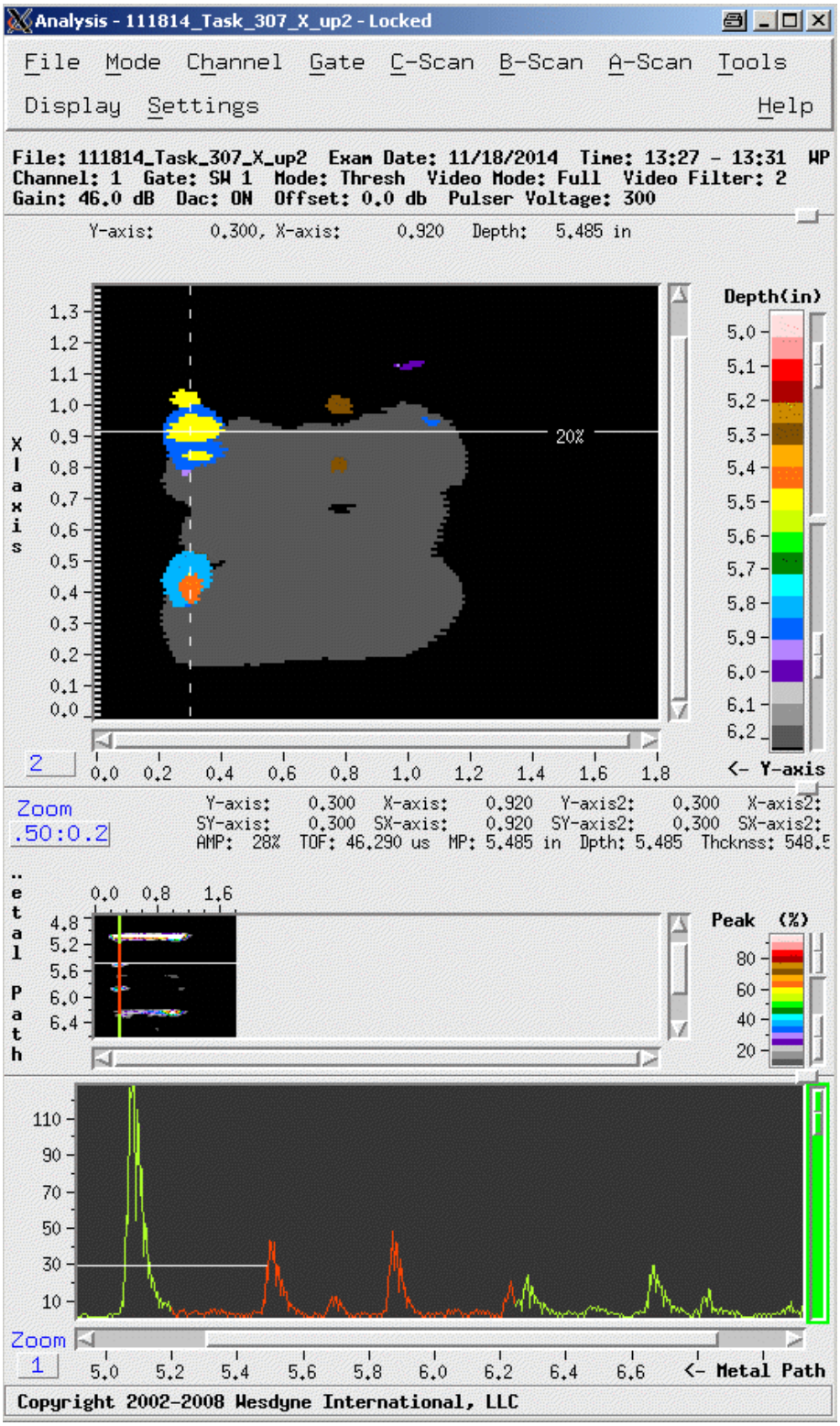

Figure 22. C-Scan output *x*-axis view, represents mostly anomaly free welds except in the upper left corner of block

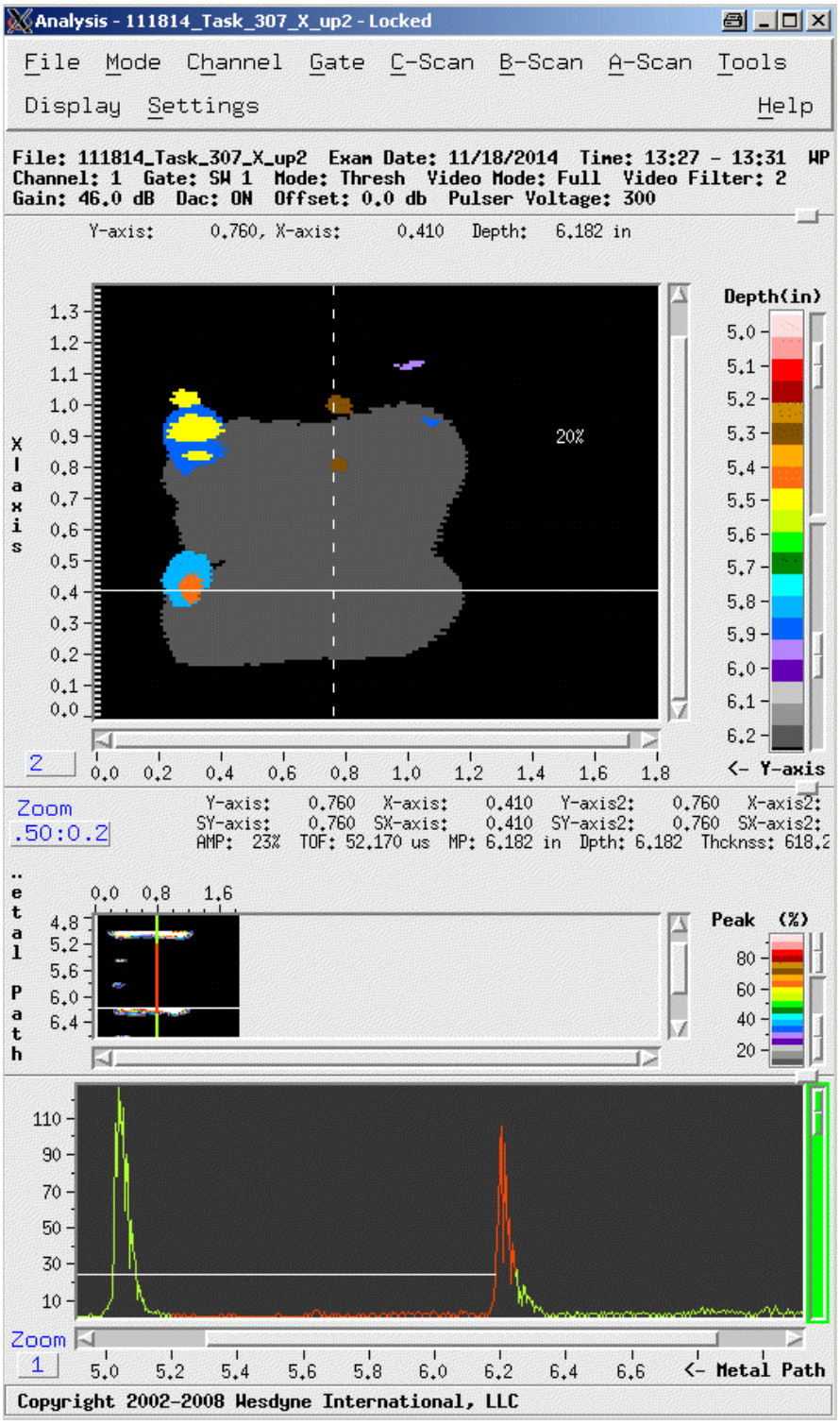

Figure 23. C-Scan output *x*-axis view, showing no anomalies in baseplate

Appendix F: Python Analysis Script

```
Pink =0
LightPink =0
Red = 0
Firebrick = 0
Goldenrod = 0
Saddlebrown = 0
Orange = 0
Coral = 0
Yellow = 0
DarkOliveGreen = 0
Green = 0
DarkGreen = 0
Cyan = 0
DeepBlueSky = 0
DodgerBlue = 0
SlateBlue = 0
DarkViolet = 0
Gray = 0
GreyShade = 0
DarkGrey = 0
Black=0
x=1
y=1
diff=5
pix = im.load()
print im.size

height,width=im.size #Get the width and hight of the image for
iterating over
print pix[x,y] #Get the RGBA Value of the a pixel of an image
 # Set the RGBA Value of the image (tuple)
Count = 0
for x in range(0,height):
     for y in range(0,width):

          value=pix[x,y]

          if ((numpy.subtract((255,220,220), value)) > -
diff).all() and ((numpy.subtract((255,220,220), value)) <
diff).all():
               Pink = Pink + 1
               Count = Count+1
          if ((numpy.subtract((253,154,154), value)) > -
diff).all() and ((numpy.subtract((253,154,154), value)) <
diff).all():

                         LightPink = LightPink+1
```

```
                            Count = Count+1

            if ((numpy.subtract((255,0,0), value)) > -diff).all()
and ((numpy.subtract((255,0,0), value)) < diff).all():
                            Red = Red+1
                            Count=Count+1

            if ((numpy.subtract((174,0,0), value)) > -diff).all()
and ((numpy.subtract((174,0,0), value)) < diff).all():
                            Firebrick = Firebrick+1
                            Count=Count+1

            if ((numpy.subtract((128,80,0), value)) > -diff).all()
and ((numpy.subtract((128,80,0), value)) < diff).all():
                            Saddlebrown = Saddlebrown+1
                            Count=Count+1

            if ((numpy.subtract((255,174,0), value)) > -
diff).all() and ((numpy.subtract((255,220,220), value)) <
diff).all():
                            Orange = Orange+1
                            Count = Count+1

            if ((numpy.subtract((255,111,16), value)) > -
diff).all() and ((numpy.subtract((255,111,16), value)) <
diff).all():
                            Coral = Coral+1
                            Count=Count+1

            if ((numpy.subtract((255,255,0), value)) > -
diff).all() and ((numpy.subtract((255,255,0), value)) <
diff).all():
                            Yellow = Yellow+1
                            Count=Count+1

            if ((numpy.subtract((205,255,0), value)) > -
diff).all() and ((numpy.subtract((205,255,0), value)) <
diff).all():
                            DarkOliveGreen = DarkOliveGreen+1
                            Count=Count+1

            if ((numpy.subtract((1,255,1), value)) > -diff).all()
and ((numpy.subtract((1,255,1), value)) < diff).all():
                            Green = Green+1
                            Count = Count+1

            if ((numpy.subtract((0,128,0), value)) > -diff).all()
and ((numpy.subtract((0,128,0), value)) < diff).all():
                            DarkGreen = DarkGreen+1
                            Count=Count+1
```

```
            if ((numpy.subtract((0,255,255), value)) > -
diff).all() and ((numpy.subtract((0,255,255), value)) <
diff).all():
                                Cyan = Cyan+1
                                Count=Count+1

            if ((numpy.subtract((0,180,251), value)) > -
diff).all() and ((numpy.subtract((0,180,251), value)) <
diff).all():
                                DeepBlueSky = DeepBlueSky+1
                                Count=Count+1

            if ((numpy.subtract((0,100,255), value)) > -
diff).all() and ((numpy.subtract((0,100,255), value)) <
diff).all():
                                DodgerBlue = DodgerBlue+1
                                Count = Count+1

            if ((numpy.subtract((180,133,255), value)) > -
diff).all() and ((numpy.subtract((180,133,255), value)) <
diff).all():
                                SlateBlue = SlateBlue+1
                                Count=Count+1

            if ((numpy.subtract((100,0,180), value)) > -
diff).all() and ((numpy.subtract((100,0,180), value)) <
diff).all():
                                DarkViolet = DarkViolet+1
                                Count=Count+1

            if ((numpy.subtract((200,200,200), value)) > -
diff).all() and ((numpy.subtract((200,200,200), value)) <
diff).all():
                                Gray = Gray+1
                                Count=Count+1

            if ((numpy.subtract((149,149,149), value)) > -
diff).all() and ((numpy.subtract((149,149,149), value)) <
diff).all():
                                GreyShade = GreyShade+1
                                Count = Count+1

            if ((numpy.subtract((88,88,88), value)) > -diff).all()
and ((numpy.subtract((88,88,88), value)) < diff).all():
                                DarkGrey = DarkGrey+1
                                Count=Count+1
            if ((numpy.subtract((0,0,0), value)) > -diff).all()
and ((numpy.subtract((0,0,0), value)) < diff).all():
                                Black = Black+1
```

```
           if x%10 == 0:
                 print
"......"+str(int(100*(float(x)/float(height))))+"%\r",


f = open(str(name)+'.txt','a')
f.write('percent of each color\n')
f.write('Gray \t'+"{:.1%}".format(float(Gray)/float(Count))+'\n')
f.write('Pink \t'+"{:.1%}".format(float(Pink)/float(Count))+'\n')
f.write('LightPink
\t'+"{:.1%}".format(float(LightPink)/float(Count))+'\n')
f.write('Red \t'+"{:.1%}".format(float(Red)/float(Count))+'\n')
f.write('Firebrick
\t'+"{:.1%}".format(float(Firebrick)/float(Count))+'\n')
f.write('Goldenrod
\t'+"{:.1%}".format(float(Goldenrod)/float(Count))+'\n')
f.write('Saddlebrown
\t'+"{:.1%}".format(float(Saddlebrown)/float(Count))+'\n')
f.write('Orange
\t'+"{:.1%}".format(float(Orange)/float(Count))+'\n')
f.write('Coral
\t'+"{:.1%}".format(float(Coral)/float(Count))+'\n')
f.write('Yellow
\t'+"{:.1%}".format(float(Yellow)/float(Count))+'\n')
f.write('DarkOlive Green
\t'+"{:.1%}".format(float(DarkOliveGreen)/float(Count))+'\n')
f.write('Green
\t'+"{:.1%}".format(float(Green)/float(Count))+'\n')
f.write('DarkGreen
\t'+"{:.1%}".format(float(DarkGreen)/float(Count))+'\n')
f.write('Cyan \t'+"{:.1%}".format(float(Cyan)/float(Count))+'\n')
f.write('DeepSkyBlue
\t'+"{:.1%}".format(float(DeepBlueSky)/float(Count))+'\n')
f.write('DodgersSuck Blue
\t'+"{:.1%}".format(float(DodgerBlue)/float(Count))+'\n')
f.write('SlateBlue
\t'+"{:.1%}".format(float(SlateBlue)/float(Count))+'\n')
f.write('DarkViolet
\t'+"{:.1%}".format(float(DarkViolet)/float(Count))+'\n')
f.write('Gray \t'+"{:.1%}".format(float(Gray)/float(Count))+'\n')
f.write('GrayShade
\t'+"{:.1%}".format(float(GreyShade)/float(Count))+'\n')
f.write('DarkGray
\t'+"{:.1%}".format(float(DarkGrey)/float(Count))+'\n')
f.write('Count \t'+str(Count)+'\n')
f.write('Black \t'+str(Black)+'\n')
f.write('Pixels in image \t'+str(width*height)+'\n')

     f.close()
```

Bibliography

Anderson, T. L. (2005). *Fracture Mechanics: Fundamentals and Applications.* Boca Raton: CRC Press.

ASTM International. (2012, March 1). Standard Terminology for Additive Manufacturing Technologies. West Conshohocken, PA, USA: ASTM International.

BBC. (2014). *Frequency, wavelength, amplitude, and wavespeed*. Retrieved December 17, 2014, from Physics: Communications using waves: http://www.bbc.co.uk/bitesize/standard/physics/telecommunications/communication_using_waves/revision/5/

Bourell, D. L., Beaman, J. J., Leu, M. C., & Rosen, D. W. (2009). A Brief History of Additive Manufacturing and the 2009 Roadmap for Additive Manufacturing: Looking Back and Looking Ahead. *US-Turkey Workshop on Rapid Technologies* (pp. 5-11). Turkish Academy.

Brown, R., Davis, J., Dobson, M., & Mallicoat, D. (2014). 3D Printing: How much will it improve the DoD Supply Chain of the Future? *XLIII* (3).

Brynjolfsson, E., & McAfee, A. (2014). *The Second Machine Age: Work, Progress, and Prosperity in a Time of Brilliant Technologies.* New York: W.W. Norton.

DaPino, M. (2014, 06 18). AFIT-OSU AM research partnership. (D. H. Gartland, Interviewer)

Dassault Systems. (n.d.). *3D CAD capabilities*. Retrieved September 24, 2014, from Solidworks: http://www.solidworks.com/sw/products/3d-cad/capabilities.htm

Dowling, N. E. (2013). *Mechanical Behavior of Materials.* New York : Pearson.

Fabrisonic LLC. (2014). *3D Printing? Additive Manufacturing?* Retrieved 05 18, 2014, from Fabrisonic: http://fabrisonic.com/technology/

Fraley, S., Oom, M., Terrien, B., & Zalewski, J. (2007, November 27). *Design of experiments via taguchi methods: orthogonal arrays*. Retrieved February 27, 2015, from The Michigan Chemical Process Dynamics and Controls Open Text Book: https://controls.engin.umich.edu/wiki/index.php/Design_of_experiments_via_taguchi_methods:_orthogonal_arrays

Freitag, D., Wohlers, T., & Philippi, T. (2003). *Rapid Prototyping: State of the Art.* Chicago: Department of Defense Information Analysis Center.

Frigon, N. L., & Matthews, D. (1997). *Practical Guide to Experimental Design.* New York: Wiley.

Gibson, I., Rosen, D. W., & Stucker, B. (2010). *Additive Manufacturing Technologies: Rapid Prototyping to irect Digital Manufacturing* . New York: Springer.

Gliner, J. A., Morgan, G. A., & Leech, N. L. (2009). *Research Methods in Applied Settings: An Integrated Approach to Design and Analysis.* New York: Routledge.

Hammer, M., & Champy, J. (2006). *Reengineering the Corporation: A Manifesto for Business Revolution.* New York: Harper Business.

International Solid Freeform Fabrication Symposium. (2009). Roadmap for Additive Manufacturing: Identifying the Future of Freeform Processing. In D. L. Bourell, M. C. Leu, & D. W. Rosen (Ed.), *International Solid Freeform Fabrication Symposium.* Austin: The University of Texas at Austin Labratory for Freeform Fabrication Advanced Manufacturing Center.

International Standard . (2001, 10 15). Industrial Automation Systems and Integration-Numerical Control of Machines-Coordinate System and Motion Nomenclature. Geneva, Switzerland: ISO.

Janaki, R. G., Yang, Y., & Stucker, B. (2006). *Effects of Process Parameters on Bond Formation During Ultrasonic Consolidation of Aluminum 3003* . New York : Journal of Manufacturing Systems.

Kane, M. (2014, July 17). LAMS Baseplate, Email message to author, July 17, 2014.

Kuhn, H. A., & Collier, K. (2014, May 12). Additive Manufacturing Processes and Materials. *American Society for Materials Interaction and America Makes* . Youngstown, OH, U.S.: America Makes.

Laufersweiler, D. C. (2014, November 26). C-Scan Questions. (D. H. Gartland, Interviewer)

MakerBot. (n.d.). *MakerBot Desktop*. Retrieved September 24, 2014, from Makerbot Products: https://www.makerbot.com/desktop

MatWeb. (n.d.). *A356.0-T6, Sand Cast*. Retrieved September 25, 2014, from MatWeb: Material Property Data: http://www.matweb.com/search/datasheet.aspx

MatWeb. (n.d.). *Aluminum 6061-T6*. Retrieved September 25, 2014, from MatWeb: Material Property Data: http://www.matweb.com/search/datasheet.aspx

Obielodan, J. O., Janaki Ram, G. D., Stucker, B. E., & Taggart, D. G. (2010). Minimizing Defects Between Adjacent Foils in Ultrasonically Consolidated Parts. *Journal of Engineering Materials and Technology* , 06-1-06-8.

Ranellucci, A. (2014). *Slic3r Features*. Retrieved September 22, 2014, from Slic3r: Gcode Generator for 3D Printers: http://slic3r.org/

Riley, W. F., Sturges, L. D., & Morris, D. H. (2002). *Statics and Mechanics of Materials: An Integrated Approach.* New York: John Wiley & Sons.

Smyth, C. (2013). *Functional Design for 3D Printing* (Vol. 1). Lexington: Clifford Smyth.

U.S. Office of Personnel Management . (2015). *Fact Sheet: How to Compute Rates of Pay.* Retrieved January 26, 2015, from U.S. Office of Personnel Management Web site: http://www.opm.gov/policy-data-oversight/pay-leave/pay-administration/fact-sheets/how-to-compute-rates-of-pay/

Ultimaker. (2013, November 02). *Cura 13.11.2 User Manual*. Retrieved September 24, 2014, from Ultimaker Support Manuals: https://www.ultimaker.com/pages/support/manuals

Valencia, V. (2013). Civil Engineering Applications of Direct Digital Manufacturing. Wright-Patterson Air Force Base, OH, U.S.A.: Air Force Institute of Technology.

Valiela, I. (2009). *Doing Science: Design, Analysis, and Communication of Scientific Research.* New York: Oxford University Press.

Weinhoffer, E. (2014). Getting Started with Slic3r. In A. K. France, *Make: 3D Printing* (pp. 45-58). Sebastapol: Maker Media.

White, D. (2000). *Patent No. 6519500.* United States of America.

Wolcott, P. L., Hehr, A., & Dapino, M. J. (2014). Optimized Welding Parameters for Al 6061 Ultrasonic Additive Manufactured Structures. *Journal of Materials Research* , 2055-2065.

Vita

Captain Daniel Gartland graduated from the United States Air Force Academy with a Bachelor of Science degree in Environmental Engineering in May 2008. He was commissioned as a Second Lieutenant in the U.S. Air Force through the Academy. He was first assigned to the 366th Civil Engineer Squadron, Mountain Home Air Force Base (AFB), Idaho. While at Mountain Home, Captain Gartland deployed to the Transit Center at Manas, Kyrgyzstan as Project Programmer for the 376th Expeditionary Civil Engineer Squadron. His second assignment was to Kunsan Air Base, Republic of Korea where he was assigned to the 8th Civil Engineer Squadron as the Chief of Operations Support. After Kunsan, Capt Gartland was assigned to Joint Base McGuire-Dix-Lakehurst (JB MDL), NJ as part of the 817th Global Mobility Readiness Squadron where he served as the Mission Support Flight Commander. During this time at JB MDL he executed pavement evaluations for Air Mobility Command (AMC) encompassing a wide range of missions including Presidential support, Force Bed-Down, and Joint level exercises. Additionally, Capt Gartland completed a Master of Science degree in Systems Engineering through Texas Tech University's distance learning program in May 2013. In August 2013, he entered the Graduate School of Engineering and Management at the Air Force Institute of Technology, where he is currently working on a Master of Science degree in Engineering Management. Capt Gartland's next assignment is to Explosive Ordinance Disposal School at Eglin Air Force Base, FL.

REPORT DOCUMENTATION PAGE

Form Approved
OMB No. 074-0188

PLEASE DO NOT RETURN YOUR FORM TO THE ABOVE ADDRESS.

1. REPORT DATE *(DD-MM-YYYY)*	2. REPORT TYPE	3. DATES COVERED *(From – To)*
Grad Date 27 Mar 2015	Master's Thesis	Aug 2013 - Mar 2015

4. TITLE AND SUBTITLE
Test and Evaluation of Ultrasonic Additive Manufacturing (UAM) for a Large Aircraft Maintenance Shelter (LAMS) Baseplate

5a. CONTRACT NUMBER

5b. GRANT NUMBER

5c. PROGRAM ELEMENT NUMBER

6. AUTHOR(S)
Gartland, Daniel H., Capt USAF

5d. PROJECT NUMBER
14V213

5e. TASK NUMBER

5f. WORK UNIT NUMBER

7. PERFORMING ORGANIZATION NAMES(S) AND ADDRESS(S)
Air Force Institute of Technology
Graduate School of Engineering and Management (AFIT/ENV)
2950 Hobson Way, Building 640
WPAFB OH 45433-8865

8. PERFORMING ORGANIZATION REPORT NUMBER
AFIT-ENV-MS-15-M-158

9. SPONSORING/MONITORING AGENCY NAME(S) AND ADDRESS(ES)
Air Force Civil Engineering Center
Dr. Joe Wander
139 Barnes Dr., Ste 1
Tyndall AFB, FL 32402
850-283-6240

10. SPONSOR/MONITOR'S ACRONYM(S)
AFCEC/CXA

11. SPONSOR/MONITOR'S REPORT NUMBER(S)

12. DISTRIBUTION/AVAILABILITY STATEMENT
Distribution Statement A: Approved for Public Release Distribution Unlimited

13. SUPPLEMENTARY NOTES
This material is declared a work of the U.S. Government and is not subject to copyright protection in the United States.

14. ABSTRACT
Additive manufacturing is an exciting new manufacturing technology that could have application to Air Force Civil Engineer (CE) operations. This research replicates a Large Area Maintenance Shelter (LAMS) baseplate design for ultrasonic additive manufacturing (UAM). Due to production problems the test section was not built as designed. Instead, a smaller block of material was submitted for evaluation. After the UAM build, ultrasonic inspection was conducted to identify anomalies in the test piece. The results of this proof of concept study indicate that UAM is not yet ready for CE expeditionary applications requiring a high degree of mechanical strength. The machine failed to build a baseplate of the same dimensions as would be required for use in the field. Further, the test specimen produced using UAM had a substantial number of anomalies throughout the entire y-axis of orientation. As the technology continues to improve, UAM may produce welds of sufficient strength to support expeditionary structural applications.

15. SUBJECT TERMS
Additive Manufacturing, Non-destructive Evaluation, Civil Engineering

16. SECURITY CLASSIFICATION OF:			17. LIMITATION OF ABSTRACT	18. NUMBER OF PAGES	19a. NAME OF RESPONSIBLE PERSON
a. REPORT	b. ABSTRACT	c. THIS PAGE			Valencia, Vhance, V., PhD, Maj, USAF
U	U	U	U	79	19b. TELEPHONE NUMBER *(Include area code)* (937) 255-3636, x 4826 (vhance.valencia@afit.edu)

Standard Form 298 (Rev. 8-98)
Prescribed by ANSI Std. Z39-18